One Earth

Article

Projected widening of sociodemographic heat disparities in the United States by end of century

Graphical abstract

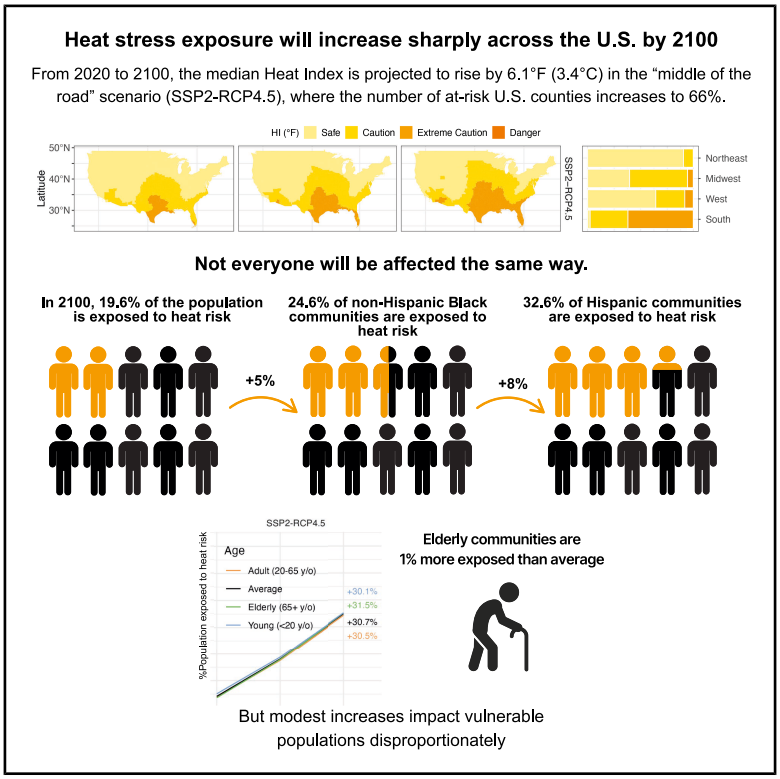

Highlights

- Heat-exposure disparities projected to widen by 2100 in the US
- Southern US, non-Hispanic Black, and the elderly face the highest heat risks
- Urgent need for targeted climate policies that consider present-day disparities

Authors

Kaihui Song, Angel Hsu, TC Chakraborty, Wei Peng, Ying Yu, Noah Kittner

Correspondence

kaihuis@berkeley.edu (K.S.), angel.hsu@unc.edu (A.H.)

In brief

We utilize Earth systems models and five future climate warming scenarios to evaluate heat stress in US counties from present day until 2100. We uncover significant disparities in future heat exposure, especially affecting the elderly and people of color, predominantly in the Southern US. Disparities for non-Hispanic Black populations are projected to widen as global temperatures rise. These results underscore the necessity of integrating sociodemographic factors in climate adaptation strategies to address heightened vulnerability and at-risk populations.

Song et al., 2026, One Earth 9, 101528
January 16, 2026
https://doi.org/10.1016/j.oneear.2025.101528

CellPress

One Earth

CellPress

Article

Projected widening of sociodemographic heat disparities in the United States by end of century

Kaihui Song,[1,*] Angel Hsu,[2,3,10,*] TC Chakraborty,[4] Wei Peng,[5,6] Ying Yu,[2,3,7] and Noah Kittner[8,9]
[1]Energy and Resources Group, University of California, Berkeley, Berkeley, CA 94720, USA
[2]Data-Driven EnviroLab, Institute for the Environment, University of North Carolina at Chapel Hill, Chapel Hill, NC 27516, USA
[3]Department of Public Policy, University of North Carolina at Chapel Hill, Chapel Hill, NC 27516, USA
[4]Pacific Northwest National Laboratory, Richland, WA 99354, USA
[5]School of Public and International Affairs, Princeton University, Princeton, NJ 08544, USA
[6]Andlinger Center for Energy and the Environment, Princeton University, Princeton, NJ 08544, USA
[7]School of Humanities and Social Science, The Chinese University of Hong Kong, Shenzhen (CUHK-Shenzhen), Shenzhen, 518172, China
[8]Department of Environmental Sciences and Engineering, Gillings School of Global Public Health, University of North Carolina at Chapel Hill, Chapel Hill, NC 27599, USA
[9]Department of City and Regional Planning, University of North Carolina at Chapel Hill, Chapel Hill, NC 27599, USA
[10]Lead contact
*Correspondence: kaihuis@berkeley.edu (K.S.), angel.hsu@unc.edu (A.H.)
https://doi.org/10.1016/j.oneear.2025.101528

SCIENCE FOR SOCIETY Extreme heat is the deadliest weather hazard in the United States (US), driving hospital visits, straining power grids, and endangering outdoor workers. However, the burden is not shared equally: race and ethnicity, age, income, and where you live shape who faces the greatest risk. Many communities still lack clear, forward-looking guidance on where temperatures and heat stress will surge and which residents will be hardest hit. Our study projects future heat exposure for every US county through 2100. We find that exposure rises everywhere, but gaps widen, especially in the South and among older adults and Black communities. State and local leaders, health departments, and utilities can use these results to target protections, such as cooling centers, home cooling assistance, shade and street trees, and worker safeguards, where they are needed most, guiding fair and effective adaptation plans.

SUMMARY

As global temperatures rise, heat-related hazards will escalate, unevenly affecting different regions and socioeconomic groups across the United States. However, we lack robust projections of who will face how much heat in the future, a gap that risks misdirecting adaptation resources and deepening avoidable and inequitable health impacts. Here, we combine multi-model ensemble of climate projections from the Coupled Model Intercomparison Project Phase 6 (CMIP6) with sociodemographic estimates to examine county-level exposure to moist heat stress from the present day to 2100. Our results show scenario-dependent widening of heat exposure by sociodemographic and geographic characteristics, with non-Hispanic Black populations, older adults, and heat-prone Southern counties experiencing the greatest increases. Across intermediate, high, and very high emission scenarios (SSP2-4.5, SSP3-7.0, and SSP5-8.5), absolute "Extreme Caution+" disparities expand, with the largest gaps in 2100 between non-Hispanic Black and non-Hispanic White populations. By resolving exposure by group, location, and scenario, these results can better inform adaptation planning that reflects differential risk and allows for prioritizing resources for the most affected communities.

INTRODUCTION

Global warming increases heat stress, which poses profound threats to human health and society,[1–5] particularly during summer months.[6,7] Recent decades have seen detrimental impacts on human health due to increased heat exposure. For instance, the contiguous United States (US) observed an increase in heat-related mortality attributed to anthropogenic climate change, with approximately 12,000 premature deaths occurring annually during the 2010s.[8,9] Increases in extreme heat stress and

resulting heat-related deaths will be greater in higher-emission future scenarios,[10] which, in addition to direct mortality and morbidity impacts of heat, will lead to a loss of agricultural productivity[11] and workplace efficiency[12,13] as well as increases in household energy consumption due to greater air-conditioning demand.[14]

There is strong evidence that such heat hazards and exposure are unevenly distributed across regions and socioeconomic groups within the US.[15] Neighborhoods with low-income and less-educated residents within a US county are exposed to significantly hotter temperatures than those with high-income and more-educated residents.[16] These differences in heat exposure have contributed to disproportionate health burdens, particularly in historically redlined areas[17] and contemporary disadvantaged communities. People of color and those living below the poverty line experience higher heat exposure and potentially more heat-related health risks than non-Hispanic White populations in wealthier areas throughout these cities.[18–22] Significant racial disparities in urban heat exposure persist in 71% of US counties even when adjusting for income.[16]

To understand how temperature and moist heat stress might evolve, Earth system models (ESMs) are widely used to project future changes in the climate and atmospheric system based on physical processes.[23,24] These models are commonly run under alternative shared socioeconomic pathways (SSPs) that are associated with different emission trajectories and, therefore, warming futures (such as different representative concentration pathways [RCPs]). When ESM outputs for projected temperature and relative humidity are combined with fine-scale SSP projections of sociodemographic features, they can, in principle, be used to assess who will be exposed to dangerous heat, where, and under which future scenarios. Existing studies have taken important steps in this direction, typically relying on downscaled climate data and overall population projections,[25] often focusing on specific geographic or sociodemographic units.[26–28] For example, Dahl et al.[26] (also see Jones et al.[29] for similar methodology) used downscaled climate models to estimate future US National Weather Service (NWS)-defined heat index (HI) exceedances relative to a 1971–2000 baseline. However, most studies do not evaluate projected impacts on multiple demographic groups simultaneously and at a spatially explicit, national scale. As a result, we still lack scenario-specific, county-scale evidence on whether heat-exposure disparities will widen or narrow for which groups and in which regions.[30] Understanding who is affected by global warming and what drives exposure disparities is therefore critical for crafting just and effective policy responses.[31]

Here, we address the limited evidence on how future climate warming will differentially increase moist heat stress across US demographic groups. We couple downscaled Coupled Model Intercomparison Project Phase 6 (CMIP6) ESM projections (2020–2100) for five SSP-RCP scenarios with socio-demographic projections for 3,108 contiguous US counties to estimate population-weighted HI exposure during summer months (June, July, and August) when heat-related risks are highest and to track how changing racial/ethnic and age structures alter future exposure under intermediate, high, and very high emission-socioeconomic pathways. This integrated climate-socioeconomic approach shows that exposure disparities widen over time, with non-Hispanic Black populations, older adults, and counties in the Southern US experiencing the largest increases in "Extreme Caution+" days. These results demonstrate that climate projections and demographic change jointly shape future heat inequities and underscore the need for adaptation strategies that explicitly prioritize socially vulnerable populations and the regions where they are concentrated.

RESULTS

Rising summer moist heat stress through 2100

To assess how warming and humidity jointly amplify future heat hazards, we first examined county-level summer (June, July, and August) HI projections under five SSP-RCP scenarios for 2020–2100. In doing so, we quantify both the magnitude and spatial distribution of future moist heat stress. Summer months are associated with higher heat-related hazards, with an even greater likelihood of heat disorders under high-emission future scenarios (Table S4).

As shown in Figure 1C, when comparing projected increases in median HI for summer months across counties under the SSP2-RCP4.5 scenario, which combines a "middle-of-the-road" socioeconomic pathway with moderate population growth and intermediate economic development aligned with countries' current climate pledges,[32] the median HI is projected to rise by 6.1°F (3.4°C) between 2020 and 2100. By 2100, under high-emission scenarios (SSP5-RCP8.5), driven by continued fossil-fuel reliance, the summer median increase in HI may reach as high as 15.0°F (8.3°C). These numbers are significantly higher than projected near-surface air temperatures between 4.2°F (2.3°C) and 9.5°F (5.3°C) for the same time period, mainly due to projected changes in relative humidity and the high sensitivity of HI to air temperature under high humidity (changes in relative humidity at the county level are detailed in Figure S4).[33] The combined impact of near-surface air temperature and humidity results in a public health risk that potentially surpasses the risk assumed when only considering the projected increase in near-surface air temperature.

When HI, rather than solely projected near-surface air temperature alone, is used, hazards rise more sharply with the inclusion of both temperature and humidity (see methods) (Figure S2). Increases in HI exceed those in near-surface air temperature, especially under higher-emission future scenarios, such as SSP3-RCP7.0 and SSP5-RCP8.5 (see county average increase in Figure 1C and county-specific percentile change in Figure S3). This pattern is most pronounced in the southern and eastern regions of the US (Figures 1A and 1B). The increases in near-surface air temperature and HI show different spatial patterns. Consistent with prior studies,[26] higher latitudes experience a greater increase in near-surface air temperature; however, HI increases are significantly higher in lower latitudes, especially in southeastern coastal areas (Figure 1D). Humidity levels play a critical role in heat perception in these areas, leading to an average increase in HI of over 3°F (1.7°C) at latitude 30° N by 2100 under the SSP2-RCP4.5 scenario. Under the high-emission scenario (SSP5-RCP8.5), changes in HI at this latitude may exceed the increase in near-surface air temperature by as much as 10°F (5.6°C). These findings suggest that residents in the South will

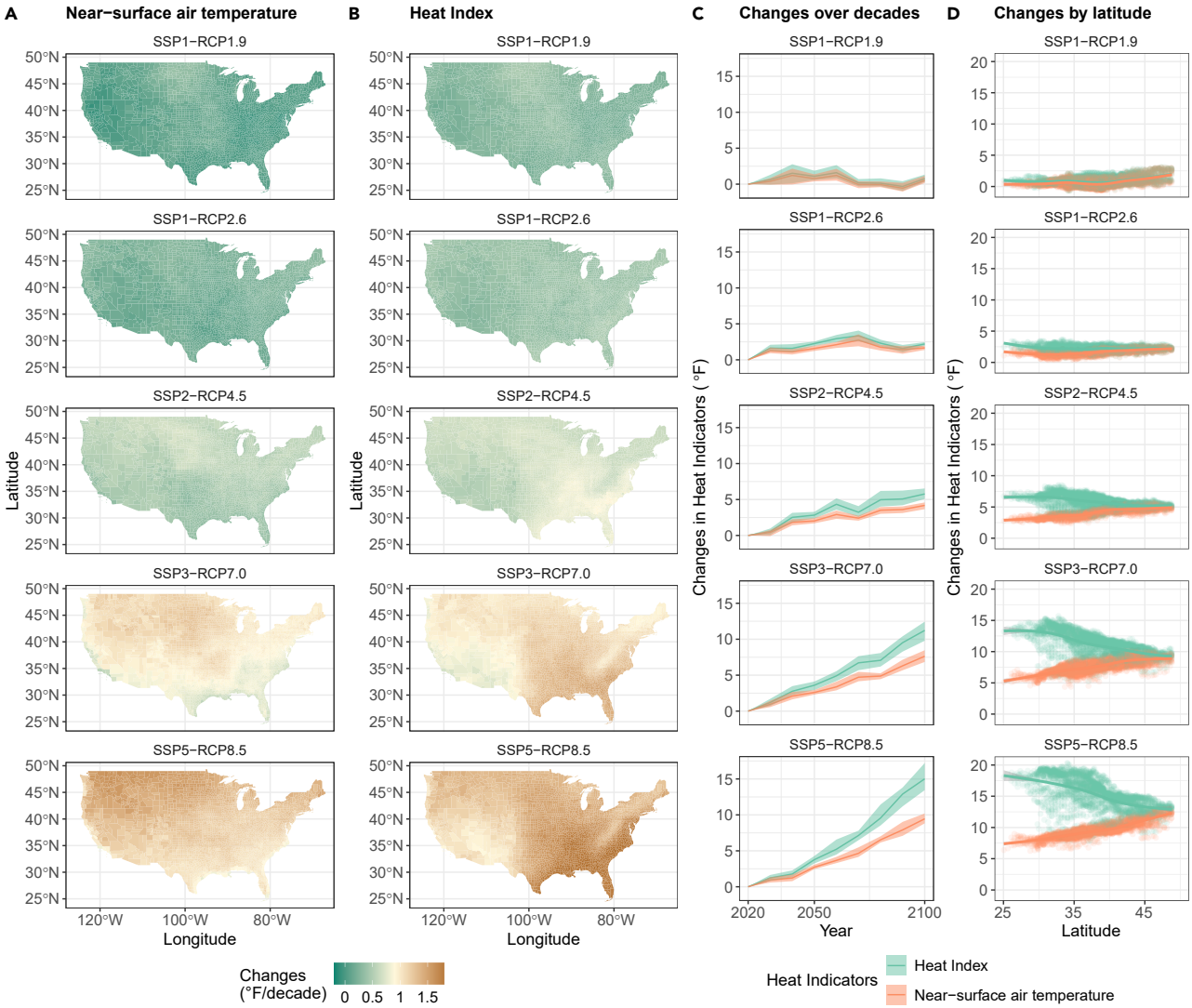

Figure 1. Projected average heat index under five coupled SSP-RCP scenarios from 2020 to 2100

(A) Per-decade changes in near-surface air temperature at the county level.

(B) Per-decade changes in heat index (HI) at the county level.

(C) Increases in heat-related indicators (near-surface air temperature vs. HI). The solid lines represent median values across various Earth system models (see supplemental methods for more details on the number of models), and the shaded areas represent values for the interquartile range.

(D) Changes in HI by latitude between 2020 and 2100. The solid line represents the median, while the shaded areas represent the interquartile range.

not only face heightened risks of heat exposure by 2100, as indicated by high absolute HI values, but also will experience a more rapid increase in HI by 2050 and 2100.

Prior research shows that 21st-century warming will increase the frequency and intensity of extreme heat events and alter the spatial pattern of daily minimum and maximum temperatures, both of which heighten heat-related health risks.[25,29,34] Since not all ESMs report daily maximum and minimum temperatures, we focus here on climate-induced disparities in summer mean HI; however, Figures S24 and S25 show that HI estimated from available daily average maximum temperatures reveals spatial patterns similar to those presented here for the monthly means, indicating that our main conclusions are robust to temporal resolution.

Spatial heterogeneity of impacts

To locate where these rising hazards concentrate, we classify counties into heat risk categories according to the NWS and assess how many people in counties move into higher-risk bins across scenarios. We group HI values using NWS thresholds categorized according to the social and health risks associated with "dangerous heat disorders with prolonged exposure and/or physical activity in the heat" (Table 1). While the recently developed national NWS HeatRisk was defined based on various considerations such as frequency, duration, and demographic characters,[35] in this article, when we refer to "risk," we are talking about the impacts of demographic groups exposed to outdoor heat hazards while assuming that vulnerability does not change substantially.

Table 1. Heat index and its relevance to public health risk

Classification	Heat index	Effect on the human body
Caution	80°F–90°F (26.7°C–32.2°C)	fatigue possible with prolonged exposure and/or physical activity
Extreme Caution	90°F–103°F (32.2°C–39.4°C)	heat stroke, heat cramps, or heat exhaustion possible with prolonged exposure and/or physical activity
Danger	103°F–124°F (39.4°C–51.1°C)	heat cramps or heat exhaustion likely, and heat stroke possible with prolonged exposure and/or physical activity
Extreme Danger	125°F (51.6°C) or higher	heat stroke highly likely

Source: US National Weather Service.

Across various future scenarios, projections indicate a substantial increase in the number of US counties facing high heat risks by mid-century and the end of the century. As shown in Figure 2A (with numeric details in Table S5), in the low-emissions scenario, following the sustainable development pathway (SSP1-RCP2.6), approximately half of US counties (50.6%) are projected to face higher risks by mid-century (2050, average across 2045–2050). This percentage rises slightly higher to 51.1% by 2100 (average across 2095–2100) compared to approximately 40% of counties at risk during the baseline period (2020, average across 2015–2020).

Under the middle-of-the-road/intermediate greenhouse gas (GHG) emissions scenario (SSP2-RCP4.5), the number of at-risk counties increases from ~40% to ~66% from the baseline period to the end of the century. By mid-century, this scenario will result in 417 counties (13.4% of total counties), home to an estimated population of around 43 million, moving from the "Safe" to "Caution" category. An additional 592 counties, where approximately 78 million people reside, will move from the "Caution" to "Extreme Caution" category by the end of the century.

The risk of prolonged heat exposure is even more pronounced in the high-emission scenario (SSP5-RCP8.5). Only 8% of the counties will stay in the "Safe" heat risk category by the 2100s, and one out of five counties in the US will be in the "Danger" category. This scenario will pose risks to 480 counties (14.9% of the total population) that will shift from the "Safe" to "Caution" category by the middle of this century, and 96.5% of these counties will be further placed in an "Extreme Caution" category by the end of this century (Table S6). These counties are mainly located in Iowa, Kentucky, and Indiana. In addition, 614 counties, mainly located in southeastern coastal states, where ~191 million people will reside by the end of this century, will face risks associated with the "Danger" category. Notably, all of these counties were initially identified as being at risk of "Caution" or "Extreme Caution" during the baseline period.

The at-risk counties are primarily located in the South census region or Southern US, encompassing a total of 17 states stretching from Texas and Oklahoma in the west to Delaware in the east. The projected HI under different future scenarios indicates elevated HI levels across the Southern US. As shown in Figure 2B, half of the population in the South will live within an "Extreme Caution" category by the end of the century under SSP2-RCP4.5 (see Table S7 for full US Census region definitions). By 2100, under the high-emission future scenario (SSP5-RCP8.5), the majority of people (97.8%) living in the Southern US will be classified as living in areas exposed to "Extreme Caution" and "Danger" heat risk categories. Even in the Northeast region, which includes nine states and where future HI is projected to be less severe than at lower latitudes due to lower relative humidity, 97.75% of the population living in this region in 2100 will experience HI values within the "Caution" and "Extreme Caution" risk categories.

Taken together, these results show that heat hazards do not expand uniformly but concentrate in specific regions, especially the Southern US, and that the number of people living in higher NWS risk categories grows across all scenarios. This analysis shows where future heat will be most consequential and provides the spatial basis for identifying future vulnerable geographies and populations.

Racial and ethnic heat-exposure disparities

To test whether the projected rise in moist heat stress will disproportionately affect racial and ethnic groups, we overlay county-level HI projections with SSP-consistent population projections for major racial and ethnic groups. We quantify disparities as the share of each group living in counties exceeding NWS thresholds for "Caution" and "Extreme Caution." We denote the two thresholds as "Caution+" and "Extreme Caution+" (HI greater than or equal to 90°F [32.2°C]). Because "Extreme Caution+" is the level at which public health warnings, early interventions, and adaptive actions become crucial, we focus on this threshold in the main text and report population-weighted HI values alongside categorical risk exposure to aid interpretation.

Baseline differences

The national population-weighted results indicate that, during the baseline period, non-Hispanic Black populations experience an average HI approximately 3°F (1.7°C) higher than non-Hispanic White populations (Table S8). This substantial absolute disparity between non-Hispanic Black and non-Hispanic White populations can largely be attributed to geographic distribution, since 57.6% of non-Hispanic Black individuals reside in the South, where HI is already high and remains consistently high across all SSP-RCP scenarios.

Disparity metrics

We evaluate disparities using two complementary measures. Absolute disparity measures the difference between a group's exposure and the overall population average, which tells us how many more people, in percentage points, from a given group are exposed to a specific heat condition. Relative disparity, on the other hand, compares a group's exposure as a ratio of the average, helping us understand how much more likely a group is to experience extreme heat compared to other groups. Together, these measures help distinguish between large population-level differences and more subtle but meaningful inequities that might otherwise be overlooked. To further explore these patterns, we mapped the percentile distribution of Hispanic (all races), non-Hispanic Black, and non-Hispanic White populations in counties experiencing HI above 90°F

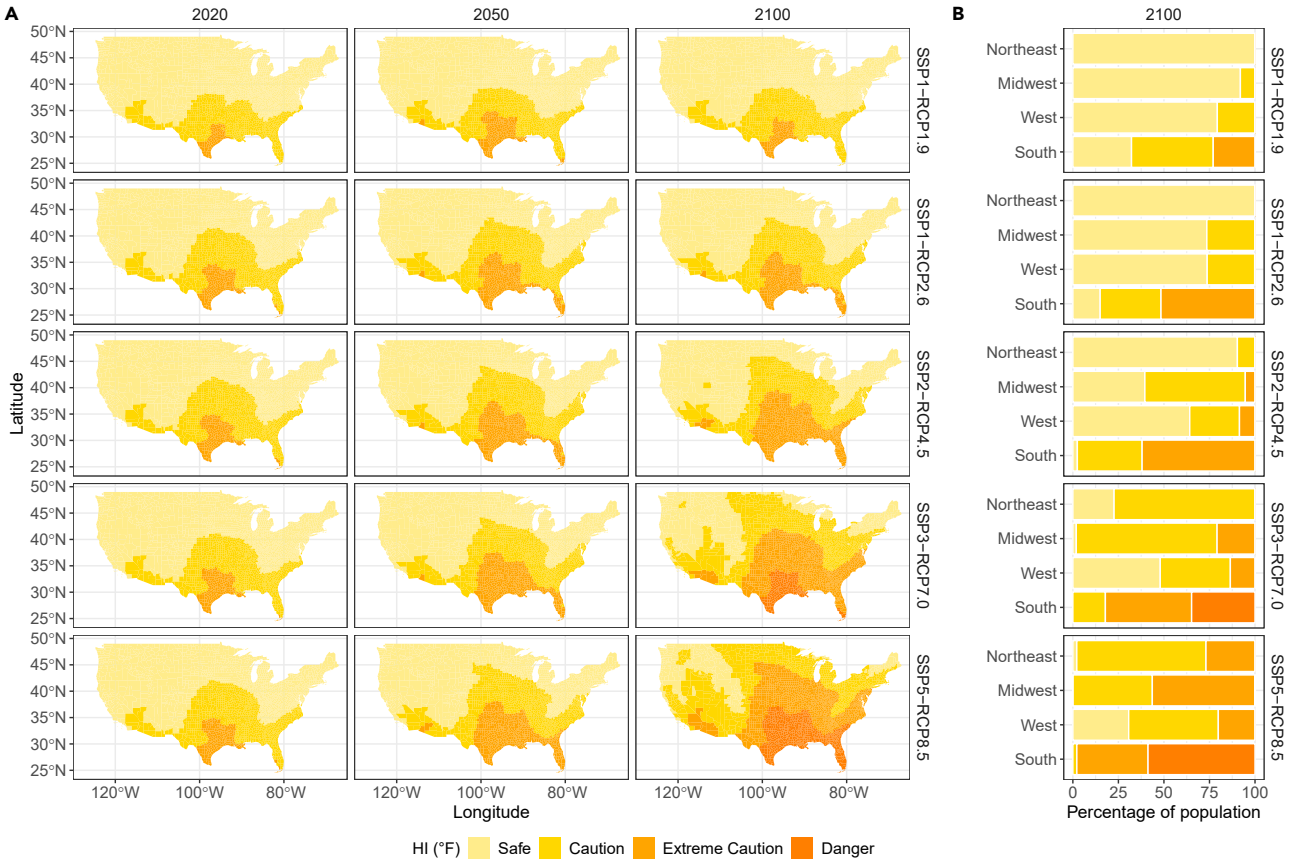

Figure 2. Projected HI, population, and counties under five future scenarios in the US

(A) Projected median HI under five future scenarios in the US (see supplemental methods for more details).

(B) Percentage of population living in the four US regions by the end of the century that will be located in areas classified as "Safe," "Caution," "Extreme Caution," and "Danger," according to the National Weather Service (NWS) HI. Note: "2020" denotes the baseline years we used for comparison (average of 2015–2020); "2050" denotes the middle of the century (average of 2045–2050); and "2100" denotes the end of the century (average of 2095–2100).

(32.2°C) ("Extreme Caution") under SSP2-RCP4.5 and SSP5-RCP8.5 scenarios in Figures S5 and S6. The results indicate that counties with higher concentrations of Hispanic and non-Hispanic Black populations are disproportionately exposed to extreme heat risks ("Extreme Caution+" risk).

Future disparities by scenario

Across SSP-RCP scenarios, we find that the overall absolute disparity increases toward the end of the century, with more pronounced increases under higher emission scenarios (Figure 3B). This upward trend is primarily driven by rising disparities among non-Hispanic Black and Hispanic (all races) populations, both of which experience above-average heat exposure (Figure 3A, with details in Figure S7). Under SSP2-RCP4.5, the proportion of Hispanic populations exposed to an HI value above "Extreme Caution" remains 6.8 to 8.3% (mean values) above the national average, reaching 37.2% vs. 30.2% for the total population by 2100 (Figure S7). Under SSP3-RCP7.0, the non-Hispanic Black exposure rises from near parity to greater than 5 percentage points above the average by 2100, and under SSP5-RCP8.5 it reaches 76.7% vs. 62.6% (a 14.1-point gap). We also assessed the sensitivity of this trend to uncertainties in future population projections and found that the direction of disparity growth remains robust, even under varying demographic trajectories.

Examining disparities in HI exposure at the lower "Caution+" threshold (Figures S9–S12) produces the same group ordering: non-Hispanic Black and Hispanic populations face greater heat exposure than the average population (Figure S10). Under the SSP2-RCP4.5 scenario, by 2050, non-Hispanic Black populations are the most disproportionately affected, with 13% higher exposure at the "Caution+" risk threshold compared to the average, followed by Hispanic populations at 5% above the average. Under the SSP2-RCP4.5, SSP3-RCP7.0, and SSP5-RCP8.5 scenarios, absolute disparity for non-Hispanic Black populations increases through mid-century and then declines toward 2100 as HI levels become universally high. Relative disparity results show the same pattern: a mid-century peak in heat-exposure disparities for non-Hispanic Black populations, followed by a later decline as everyone is exposed.

Absolute vs. relative patterns

As HI exposure becomes widespread, overall relative disparity declines (Figure 3D), largely due to the near-universal increase in HI across all populations. However, this trend does not imply inequity declines, since the absolute number and share of

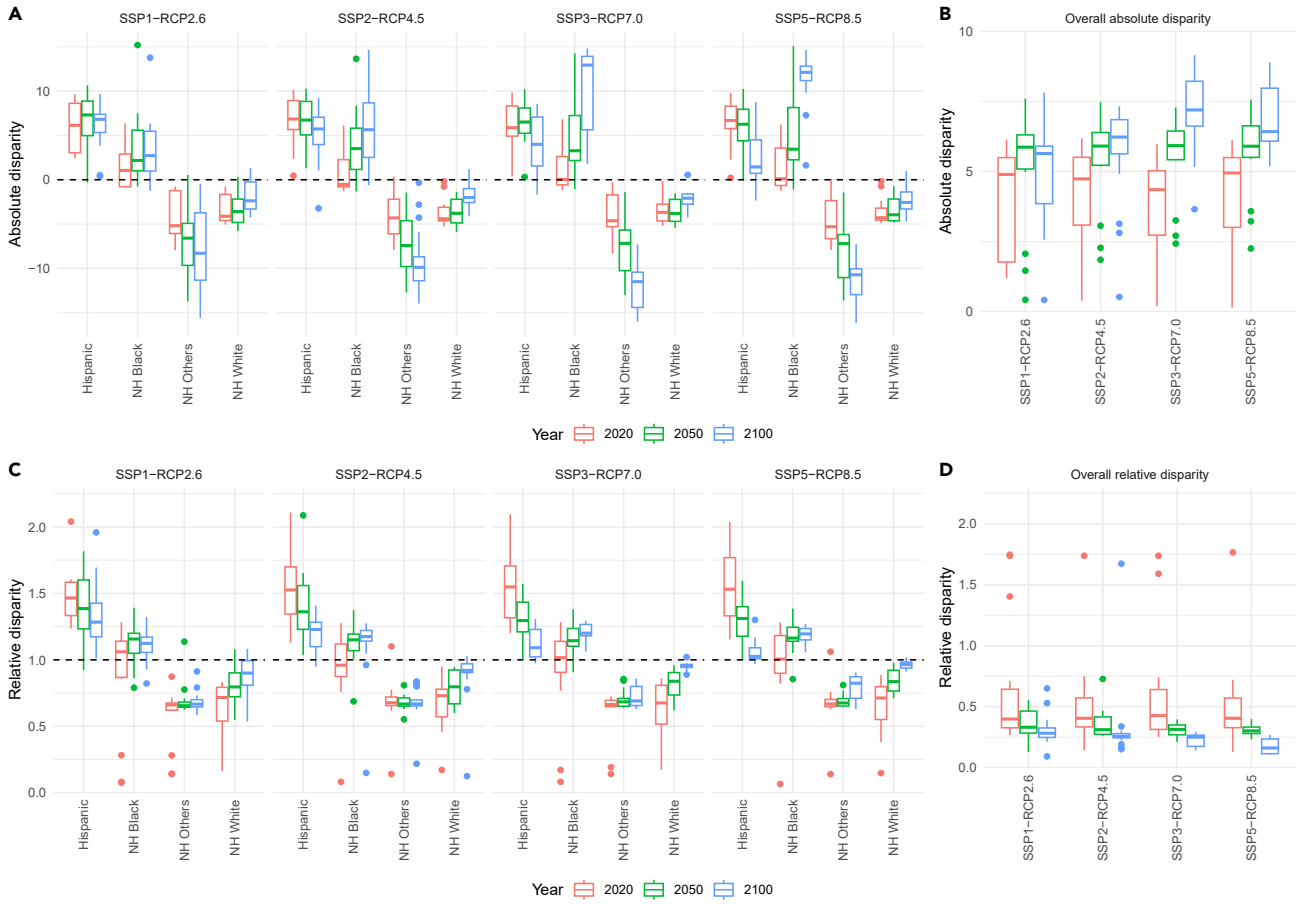

Figure 3. Racial/ethnicity disparity in exposure to HI above "Extreme Caution" threshold under future scenarios

(A) Absolute disparity of racial-ethnicity groups in exposure to HI above "Extreme Caution" threshold (HI ≥90°F [32.2°C]) under future scenarios.

(B) Overall absolute disparity in exposure to HI above "Extreme Caution" threshold under future scenarios.

(C) Relative disparity of racial-ethnicity groups in exposure to HI above "Extreme Caution" threshold under future scenarios.

(D) Overall relative disparity of racial-ethnicity groups in exposure to HI above "Extreme Caution" threshold under future scenarios.

Absolute disparity is measured as the difference between a group's exposure and the overall population average, while relative disparity represents the ratio of a group's exposure to the population average. Hispanic, Hispanic (all races); NH-Black, non-Hispanic Black; NH-White, non-Hispanic White; NH-Others, non-Hispanic other races. Each boxplot shows the interquartile range (IQR) (25th–75th percentile), with the median indicated by a horizontal line. Whiskers extend to 1.5× the IQR, and points beyond the whiskers are plotted as outliers. See supplemental methods for more details on the number of models. The black dashed lines represent benchmark values for perfect equalization.

non-Hispanic Black and Hispanic residents in high-risk counties continue to rise. In fact, the group-specific relative disparity for non-Hispanic Black populations continues to increase (Figure 3C), especially in higher-emission scenarios. Conversely, non-Hispanic other races (including Native American, Native Hawaiian, and Asian populations) consistently have the lowest exposure to "Extreme Caution+" risk across all SSP-RCP scenarios.

Spatial concentration within the non-Hispanic Black population

To examine whether these disparities are being driven by where non-Hispanic Black populations reside, we compared counties in the top and bottom quartiles of non-Hispanic Black population share (Figure 4 and Table S9). These results show that an increasing proportion of the non-Hispanic Black population, particularly in counties with higher non-Hispanic Black population shares, is at greater risk across time and under more extreme SSP scenarios (e.g., SSP3-RCP7.0 or SSP5-RCP8.5). In 2020, the proportion of counties exceeding "Safe" thresholds is relatively low across all SSP scenarios, with SSP1-RCP2.6 showing that only 13% of the counties with the highest shares of non-Hispanic Black populations (i.e., top quartile) reach a level of summer HI exposure levels where extreme caution is advised. By 2050, the risk increases significantly, with SSP3-RCP7.0 showing 32% of counties in the top quartile exceed even more critical heat thresholds advising extreme caution, indicating severe heat conditions that pose health risks. This substantial increase suggests an escalating trend of growing vulnerability to extreme heat by mid-century. The trend continues starkly into 2100, where the SSP5-RCP8.5 scenario shows extreme peaks, with up to 78% of counties in the top quartile falling into the "Danger" category of the HI, indicating that an overwhelming majority of the non-Hispanic Black populations in these counties could

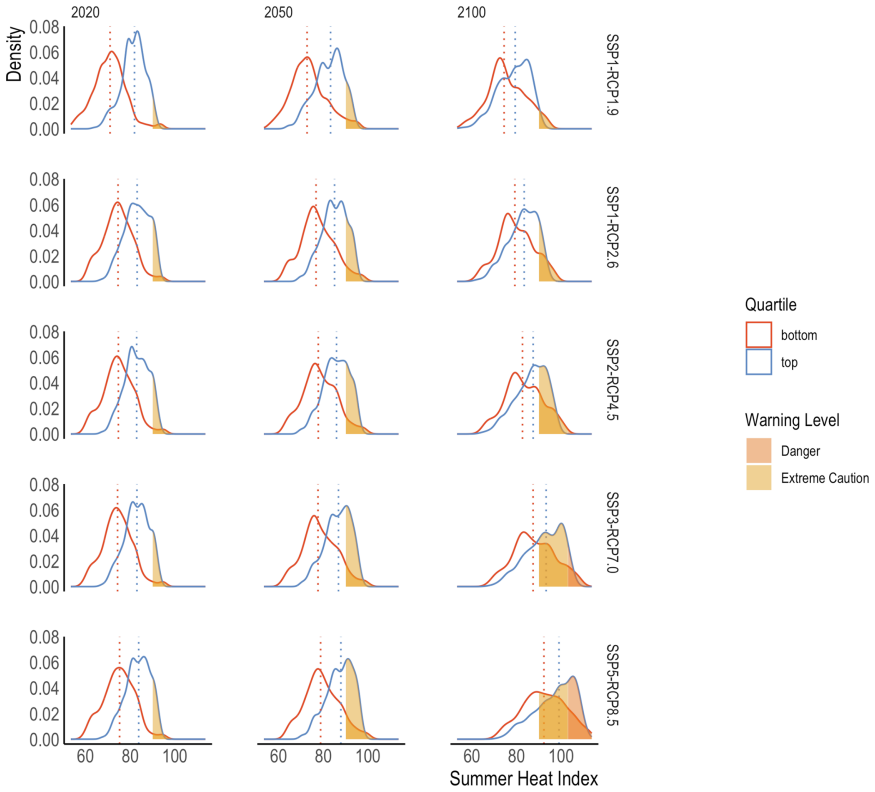

Figure 4. Distribution of summer HI under various SSP-RCP scenarios for non-Hispanic Black populations in US counties from 2020 to 2100

Top and bottom quartiles represent the counties with the highest and lowest proportions of non-Hispanic Black population out of the county's total population, respectively.

experience severe heat stress, far surpassing other SSP scenarios in terms of risk and potential health impacts.

These results show that racial and ethnic disparities observed at baseline persist across thresholds ("Caution+" and "Extreme Caution+") widen in absolute terms for non-Hispanic Black and Hispanic populations, especially under higher-emission scenarios, and are magnified in counties with high concentrations of these groups.

Age-related disparities in heat stress exposure

To assess whether population aging will interact with spatially concentrated heat to create additional health-relevant inequities, we analyze heat exposure for three age groups—young (<20 years), adult (20–64 years), and elderly (≥65 years)—across four coupled SSP-RCP scenarios. We explore disparities in exposure to "Extreme Caution" heat levels, focusing on changes in absolute and relative disparities over time (Figure 5, with further details in Figures S13 and S14). Our results highlight that elderly individuals (age ≥65) currently experience lower HI than the average population (Figure 5A). However, in the future, HI values are projected to rise approximately 0.2°F (0.1°C) higher than for adults (see Table S10 for population-weighted HI). While population-weighted HI exposure does not vary drastically by age group at the national scale (Table S10), our expanded analysis of subnational regions reveals that localized elevation of the exposure among elderly adults occurs in some regions, particularly in warmer southern states. Furthermore, the same level of HI poses greater health risks for the elderly, due to diminished thermoregulatory capacity and a higher prevalence of chronic illness.[36,37] Figure S15 illustrates age-stratified trends in HI exposure over time, showing modest but persistent increases in exposure for elderly populations under all scenarios. Since elderly populations are more vulnerable to heat-related health risks, this increase in HI may heighten the risk of heat-related illnesses and mortality.[38]

By the end of the century, counties in Florida, Texas, and coastal South Carolina, where a large proportion of the elderly populations reside, are expected to be exposed to "Extreme Caution" heat risks (Figures S13 and S14). The elderly population is projected to experience a slightly higher relative exposure to heat stress compared to the overall population under the SSP2-RCP4.5 scenario (~1% above the average; Figure 5C). While this difference is small in magnitude, it aligns with a broader trend of increasing heat burden for aging populations, where even modest increases in exposure could have disproportionate health impacts. Currently, the young population (<20 years old) experiences slightly higher exposure to HI above "Extreme Caution" (about 1% above the average), but this disparity decreases across all scenarios over time (Figure 5D). Similar trends are observed in HI exposure above the "Caution" threshold, where the elderly populations are increasingly affected by heat risks (Figures S16–S19). Age composition by HI category is shown in Figure S20.

Overall, age-related disparities are small at the national scale but become meaningful in regions where elderly populations and high HI co-occur.

DISCUSSION

This study addresses an unresolved question in the heat climate literature: as US temperatures and humidity increase, will disparities in heat exposure across sociodemographic groups diminish because exposure becomes widespread or intensify because populations already located in hotter, more humid regions experience the largest additional burdens? Prior studies have been limited to specific geographies, single population groups, or a narrow set of scenarios, making it difficult to assess how exposure evolves simultaneously across major racial and ethnic groups and across all US counties. By combining CMIP6 projections of temperature and humidity with county-level, SSP-consistent demographic projections for the contiguous US, we provide a scenario-resolved, spatially explicit characterization of who is exposed, where, and under which future pathways.

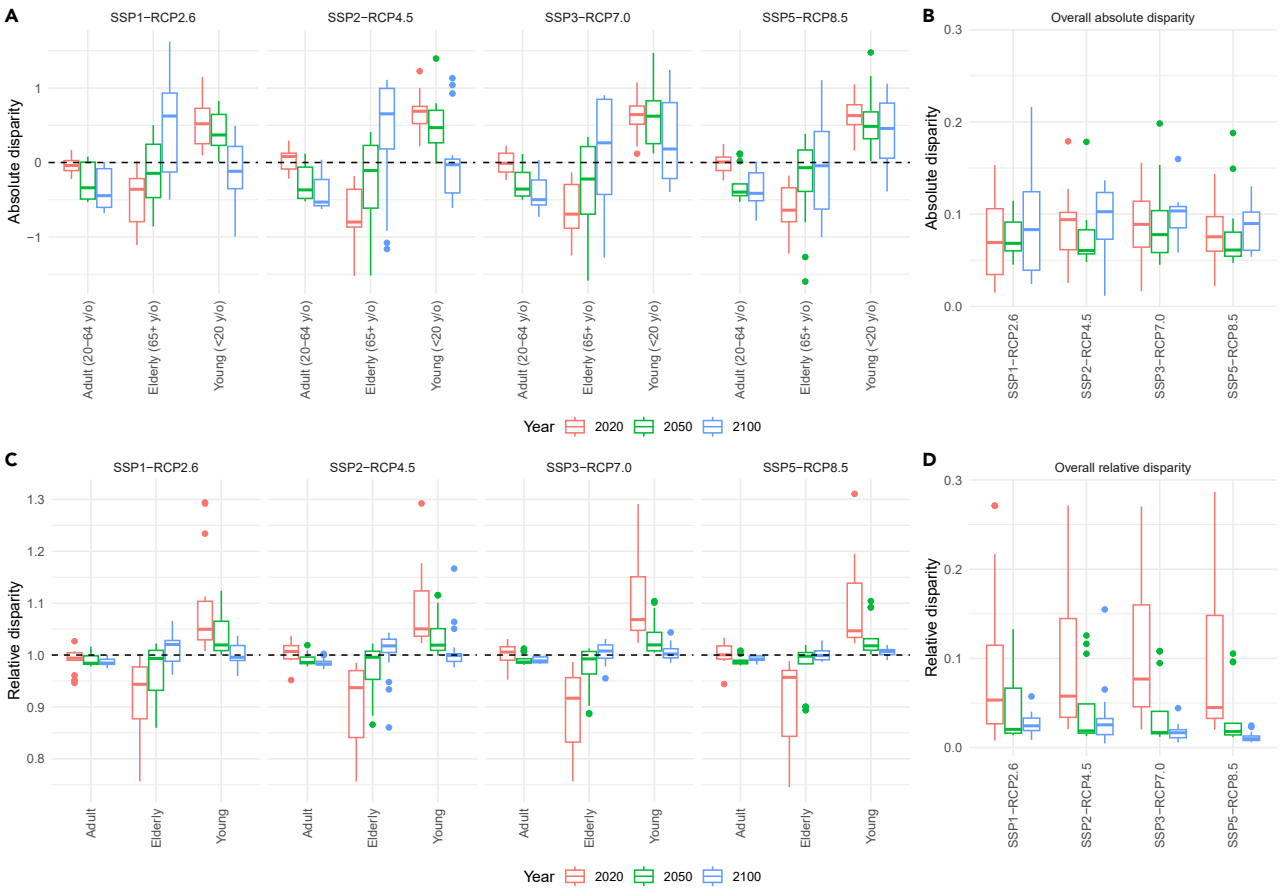

Figure 5. Age disparity in exposure to HI above "Extreme Caution" threshold

(A) Absolute disparity and relative disparity of age groups in exposure to HI above "Extreme Caution" threshold under future scenarios.

(B) Overall absolute disparity of age groups in exposure to HI above "Extreme Caution" threshold (HI ≥90°F [32.2°C]) under future scenarios.

(C) Relative disparity of age groups in exposure to HI above "Extreme Caution" threshold under future scenarios.

(D) Overall relative disparity of age groups in exposure to HI above "Extreme Caution" threshold under future scenarios.

Each boxplot shows the IQR (25th–75th percentile), with the median indicated by a horizontal line. Whiskers extend to 1.5× the IQR, and points beyond the whiskers are plotted as outliers. See supplemental methods for more details on the number of models. The black dashed lines represent benchmark values for perfect equalization.

Our findings indicate that Southern US counties, with the largest percentage of people of color, specifically non-Hispanic Black communities, will likely encounter the most substantial HI increases over time and experience the most significant absolute increases when compared to other demographic groups, particularly non-Hispanic White populations. In terms of age, populations over the age of 65 may be disproportionately exposed to increased HI levels when compared to populations under the age of 65 in every scenario examined. As the climate continues to warm, which is a trend observed across all SSP-RCP scenarios, higher temperatures will not be confined to the summer months but will extend into other parts of the year.[39] This prolonged heat exposure could further exacerbate health risks, particularly for vulnerable populations, especially the elderly and people of color who face a higher likelihood of heat-related illness[40] and are already experiencing sustained high HI levels. These results underscore the need for understanding differences in underlying sociodemographic factors when evaluating future heat impacts and temperature changes due to climate change. We now discuss three considerations when applying these results to future studies or policy applications.

The Southern US is most vulnerable to rising heat risks

Our findings consistently demonstrate that HI in the Southern US remains persistently high across different future scenarios up until 2100. Although SSPs do not explicitly account for migration and that racial, ethnic, and age groups may substantially shift their location from present-day patterns, our results show that consistent patterns of heat exposure persist across demographic groups under different SSP scenarios. The counties with the highest HI increase are collocated with counties with higher percentages of non-Hispanic Black populations and people over the age of 65 across different SSP-RCP scenarios. However, our results still represent a conservative estimation, since we use the monthly average HI. Extreme-heat days, which can exceed several standard deviations above the monthly average HI, have the potential to pose even greater risks and, thus,

potential disparities in outcomes, within a few days.[23] Additionally, impacts of heat exposure are highly context dependent, particularly in heterogeneous urban environments, where local urban design (such as the shade of buildings or trees) or availability of air conditioning plays a critical role in individuals' perception of heat stress.[20,24,39]

Our estimation shows geographic overlaps between increases in HI and vulnerable demographics for both race and age, particularly in the Southern US, where the majority of the US non-Hispanic Black population and elderly are located. These demographic groups are well documented to be more vulnerable to heat exposure, in part due to compounding factors such as lower socioeconomic status, which is more prevalent in the Southern US and has been linked to greater health risks in previous studies.[7,41,42] Our disparity analysis reveals that HI increases will disproportionately affect non-Hispanic Black populations compared to other racial groups. Furthermore, in the worst-case climate warming scenarios, the gap between HI increases for non-Hispanic Black populations and non-Hispanic White populations widens over time. Other racial and ethnic groups do experience a smaller HI disparity gap compared to non-Hispanic White populations, and this gap narrows in the future in every scenario examined. Further analysis of heat disparity across regions reveals that both absolute and relative disparities by racial/ethnic group in the South decline toward the end of the century, as the HI remains uniformly high across the region. In contrast, the West experiences the most significant increase in disparity, particularly under the high-emission scenario (SSP5-RCP8.5) (Figures S21–S24).

Regarding age, our study highlights a growing disparity in heat exposure between individuals aged 65 and older and those younger than 65, emphasizing the increasing HI and heat exposure among more vulnerable elderly populations. Existing studies have found that "people aged 65+ have been several times more likely to die from heat-related cardiovascular disease than the general population."[43] This finding underscores the critical need for prioritizing climate adaptation and mitigation strategies for elderly people, who stand to be at a greater risk of heat-related health effects due to increased exposure to HI when compared with their younger, healthier counterparts.[5,44]

Incorporating equity considerations into adaptation

The findings of our study highlight a consistent demographic disparity in future heat exposure, revealing greater and growing gaps in exposure for non-Hispanic Black populations and the elderly, particularly in the Southern US, across all future scenarios, even with a conservative estimation based on monthly HI. Our analyses did not consider the adoption of additional adaptation measures, such as air conditioning and aggressive greening, and assumed no changes in vulnerability (e.g., other underlying health conditions that may become more chronic under climate change). These measures, such as air conditioning[45] and green space,[46] have been shown to be distributed unequally among populations both in and outside of urban areas. Implementing preventive measures to address these heat-exposure and adaptively measuring disparities is critical to shape future climate policies to address what Frosch et al. refer to as the "climate gap," in which African American and Latino communities already face disproportionate health and economic consequences due to climate and environmental hazards.[47] In addition, statistics also show that labor-intensive outdoor industries—such as construction, landscaping, and logistics[48,49]—are primarily located in the South,[50,51] potentially posing higher health risks to labor forces and economic loss to society.[52,53]

Analysis of mid- and long-term impacts of climate-related heat exposure on different socioeconomic groups is crucial to the development of adaptation plans at the local scale. According to Malloy and Ashcraft,[54] since just adaptation planning requires the inclusion of socially vulnerable populations, knowing where and whom these populations are is critical to engaging them in processes that ensure their involvement in planning decisions that ultimately affect them. The Inflation Reduction Act allocated substantial funding for environmental and climate justice, positioning cities and states to support underserved communities.[55] Recent uncertainties in fund distribution highlight the need for sustained local engagement.

Limitations of seasonal focus and applying ESMs to understand future heat stress

Our primary analysis focuses on the summer months (June, July, and August) when heat exposure is most intense and health risks are typically highest. This seasonal focus is consistent with prior research,[10–12] which identifies these months as experiencing the greatest increases in temperature extremes and cumulative heat stress, compounded by already elevated baseline HI values. However, we acknowledge that this approach may underestimate total annual heat exposure, particularly as extreme heat events are increasingly occurring outside the traditional summer season. For example, anomalous heatwaves in September or earlier onset in May have been documented in recent years, potentially exposing vulnerable populations to substantial risk. To account for such year-round events, some studies adopt annualized measures such as person-days of exposure.[13] While our analysis does not capture these off-season events, we believe the summer-focused approach offers a robust, policy-relevant baseline for evaluating acute heat risk.

Moreover, our study utilizes county-level averages of HI due to the coarse resolution (~100 km, see Table S2) of ESM spatial grids, which are often larger than individual counties. These grids limit our ability to capture fine-scale spatial variations in heat stress that would be more relevant for furthering the analysis of disparities. This limitation is particularly salient in the context of urbanization, where microclimates within cities can lead to localized areas with significantly higher heat exposure compared to surrounding rural areas.[56,57] ESMs lack the resolution, and even appropriate urban representations, to capture these urban heat islands, which potentially leads to an underestimation of localized heat exposure in urban areas. While mesoscale models have been recently used to demonstrate pervasive historical and present-day disparities in moist heat stress within US cities,[17] similar future projections that account for both future urban growth and resolve the projected evolution of urban neighborhood-scale characteristics are currently unavailable. This will be an important consideration to more accurately quantifying potential disparities in human impacts due to future warming on an increasingly urbanizing planet. Moreover, these estimates all relate to outdoor hazard and potential exposure, and overall risk in the present and the future would also depend on the time spent indoors vs. outdoors among different relevant

populations and their vulnerabilities.[58] Currently, there are substantial race- and income-based disparities in exposure and vulnerability, including the nature of workplaces and air-conditioning access, in the US,[45] which would underestimate the heat-related risks if only based on estimates of outdoor hazard.

Our analysis only focuses on monthly summertime average HI, when heat hazards are most intensive and with the largest increases (see Figure S27 for all months). We acknowledge that this seasonal focus presents certain limitations. While this measure provides a valuable long-term climatological perspective on future climate change, extreme heat events have more acute impacts on human health.[5] While US counties and regions experiencing the highest heat stress due to these extreme events are likely to remain consistent, the disparities between populations living in these areas and others may become more pronounced when considering sub-daily fluctuations in heat stress and multi-day sustained exposure to high ambient heat stress. With all that being said, our results confirm that global mean air temperature change is non-linearly related to moist heat stress change under warming scenarios, meaning that the same future warming experienced could trigger larger increases in societal and health impacts than expected when only using air temperature.[59]

Physical model uncertainties

When utilizing future climate projections from ESMs, it is important to be cognizant of various sources of uncertainties, including those in the underlying model (parametric and structural uncertainties) as well as the scenarios (scenario uncertainty). While measures in standardizing inputs across various ESMs were taken to enhance the comparability of model outputs,[60] the differences in outputs are still influenced by parametric uncertainty and model structural uncertainty.[61] In our analyses, we employ an ensemble of model results to consider the uncertainty range arising from model choice and implementations, although it does not mitigate the overall uncertainty. Additionally, the projections of sociodemographic changes under different SSPs introduce further uncertainty. These SSPs, widely used in scientific assessments like the IPCC Sixth Assessment Report, outline five distinct future socioeconomic scenarios, each paired with a demographic and economic narrative and relevant assumptions (Table S1). In our study, we pair each macro-level SSP-RCP scenario used by ESMs with a set of fine-scale projections of SSPs (Figure 6). This allows us to explore how varying assumptions about population growth, economic productivity, and GHG emissions influence the resulting heat stress projections and exposure disparities. After 2050, these projections diverge significantly, highlighting the increased uncertainty in projecting population growth and economic activities far into the future, alongside varying assumptions about equilibrium climate sensitivity across models.[61]

Even with bias-corrected datasets, uncertainties in future climate projections remain large due to several factors. Bias correction, which typically involves adjusting present-day climate model outputs to match observational or reanalysis datasets (such as ERA5), helps align historical simulations with observed conditions. However, applying a fixed offset to bias correct all future projections assumes that model biases remain constant over time, which may not hold true given changes in climate dynamics, feedback mechanisms, and model parameterizations. Bias correction could even introduce additional uncertainties, as previous studies observe,[62] which can amplify errors, particularly if biases vary non-linearly across different areas. Therefore, while bias correction may shift the absolute magnitude of projected HI values, it is unlikely to alter our analysis of the direction of disparities and trends highlighted in our study. Since our primary focus is on understanding relative differences in heat exposure across demographic groups and geographic regions rather than absolute temperature values, bias correction may not meaningfully change our key findings. Instead, our ensemble approach ensures that projected trends remain robust to the underlying uncertainties in the climate model outputs.

Uncertainties in future population projections

Precisely projecting heat-related impacts and inequality is even more challenging. Most SSPs are developed at the global scale with energy and emission scenarios developed with regional or national-level population projections. National or state-level HI projections are insufficient to analyze demographic disparities between different geographic populations. While scholars have developed methodologies and techniques to downscale demographic composition to higher spatial resolutions,[63] making high-resolution projections (e.g., census block level) is intrinsically uncertain due to the additional assumptions needed in the downscaling process. Thus, analyzing demographic patterns at higher spatial resolutions, such as census tract or census block level, is impeded by data constraints.

METHODS

Data description

Climate projections

Future climate projections were obtained from the Scenario Model Intercomparison Project (ScenarioMIP) within the CMIP6. We calculated the median values of HI, a moist heat stress index used operationally by the NWS, at the standard 100-km resolution from 26 global climate and ESMs for five SSP-RCP scenarios based on the model-simulated near-surface air temperature (*tas*) and relative humidity (*hurs*). To do this, monthly median *tas* and *hurs* were first extracted from all the models and then averaged across the summer months to obtain a June, July, and August (JJA) averaged HI. We then took the median values from the multi-model ensemble to reduce the uncertainty associated with model choice.

Figure S1 illustrates four tier 1 coupled SSP-RCP scenarios (i.e., top priority scenarios modelers have identified that represent a wide spectrum of uncertainty in future socioeconomic and climate forcing pathways) and an additional SSP1-RCP1.9 scenario (a scenario designed to limit global warming to 1.5°C above the temperature in 1850–1900) that we focus on in this study. ESMs use SSP-RCP emission scenarios from global integrated assessment models that rely on regional/national-level socioeconomic and technological projections. These projections generate global and regional GHG emissions, which are then downscaled based on present-day spatial patterns and used as inputs to ESMs. The ESMs, in turn, simulate future climate variables such as temperature and humidity, which we use to estimate the HI. The models used to project the HI are listed in Table S2. We analyze the disparity of heat stress in the

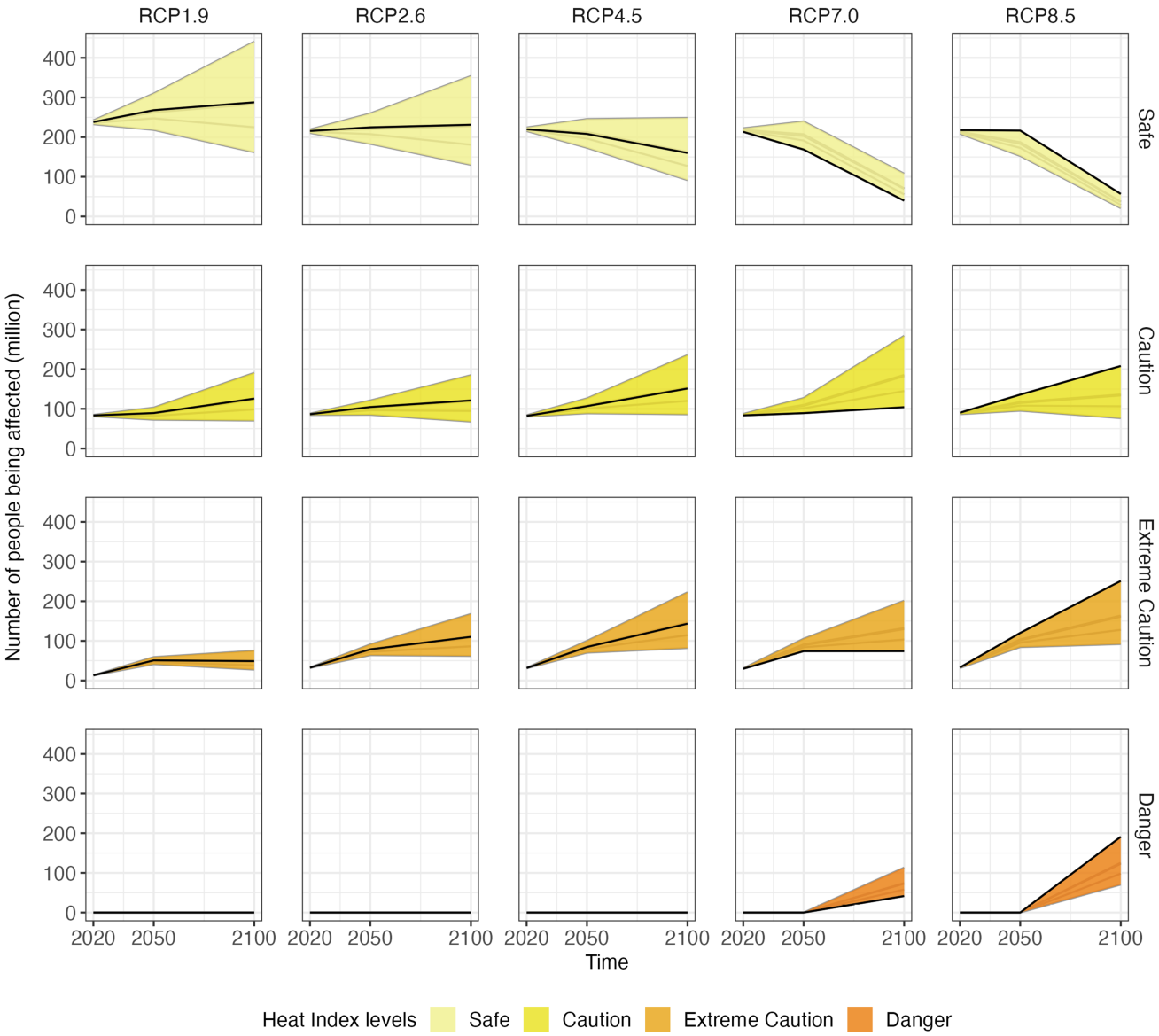

Figure 6. Projected total number of people affected by heat stress from 2020 to 2100

The black lines represent the most likely coupled SSP-RCP scenarios (SSP1-RCP1.9, SSP1-RCP2.6, SSP2-RCP4.5, SSP3-RCP7.0, and SSP5-RCP8.5), while gray lines denote projections under other possible coupled scenarios, highlighting the variability and potential range of outcomes.

baseline period (denoted as 2020, using the mean of 2015–2020), middle-of-the-century period (denoted as 2050, using the mean of 2045–2050), and end-of-the-century period (denoted as 2100, using the mean of 2095–2100).

Socioeconomic data

Multiple research efforts have developed fine-scale (e.g., county-level) sociodemographic projections aligned with SSP narratives. SSPs not only serve as macro-level drivers of GHG emissions that feed into climate models but also provide micro-level demographic patterns essential for assessing disparities in heat exposure. We used these fine-scale sociodemographic projections to combine with HIs to analyze disparities in projected heat exposure. To assess the potential impacts of projected moist heat hazards on different populations, we obtained socioeconomic data, including total population and gender, race, and age groups from multiple sources consistent with the SSPs considered in our study at finer spatial resolution (see Table S3 for details). We then aggregated the downscaled socioeconomic data into the county level to analyze the potential outdoor exposure of different socioeconomic groups to future heat stress. Given the challenges in downscaling and extrapolating GDP data for the SSPs,[64] we did not examine future disparities between different income groups.

Heat index

Heat stress indices, which typically combine several factors modulating human heat loading, including air temperature

and humidity, can better inform the impact of heat on the human body than air temperature alone. Here, we employ a moist heat stress index because of its relevance to increasing morbidity and mortality risk as a consequence of global warming, which would also be associated with changes in humidity.[8,65] Among the wide array of over 20 different heat indices in the literature, we chose to use the NWS HI, which is a moist heat stress index used by the NWS to measure how hot it "feels" to the human body (see supplemental information for more details).[66,67] The NWS HI is based on Steadman's apparent temperature. Based on Steadman's theory, Rothfusz performed multiple regression analyses, described in a 1990 NWS Technical Attachment (SR 90-23).[66,67] This HI is widely used in heat warning systems and environmental health research, and the relevant health risk categories, most frequently exceeded and relevant for the Southern and Southeastern US, are shown in Table 1. For ease of comparability, we use the same threshold for all regions in our analysis.

This HI is a function of air temperature and relative humidity. In our study, we use the projected near-surface temperature (*tas*) and projected surface relative humidity (*hurs*) derived from multiple CMIP6 models to calculate HI under different climate change scenarios. The calculation of HI is performed using the R package weathermetrics developed by Anderson et al.[66]

$$\begin{aligned} HI = & -42.379 + 2.04901523tas + 10.14333127hurs \\ & - 0.22475541tas \times hurs - \left(6.83783 \times 10^{-3}\right)tas \\ & - \left(5.481717 \times 10^{-2}\right)hurs + \left(1.22874 \times 10^{-3}\right)tas \\ & \times hurs + \left(8.5282 \times 10^{-4}\right)tas \times hurs \\ & - \left(1.99 \times 10^{-6}\right)tas \times hurs. \end{aligned}$$

If *hurs* is 13% or less and *tas* is between 80°F (26.7°C) and 112°F (44.4°C),

$$HI = HI - \left(\frac{13 - hurs}{4}\right) \cdot \sqrt{\frac{17 - |tas - 95|}{17}}. \quad \text{(Equation 1)}$$

If *hurs* is over 85% and *tas* is between 80°F (26.7°C) and 87°F (30.5°C),

$$HI = HI + \left(\frac{hurs - 85}{10}\right) \cdot \sqrt{\frac{87 - tas}{5.}} \quad \text{(Equation 2)}$$

Disparity metrics

We used absolute disparity and relative disparity to measure disparity in heat exposure by racial groups and age groups. The absolute disparity is calculated as the HI difference between demographic groups and, similarly, the relative disparity is calculated using the ratio between demographic groups. Specifically, the racial disparity measures the disparity of non-Hispanic Black, Hispanic (all races), and non-Hispanic other races against the non-Hispanic White population, while the age disparity measures the disparity of the elderly population (age ≥65) and the young population (age <20) against the adult group (age 20–65). The absolute and relative disparities have been used in many studies[10,68–70] to measure sociodemographic differences.

The absolute disparity for a given year is calculated as

$$\text{Absolute disparity of a demographic group} = q_i - \mu(q), \quad \text{(Equation 3)}$$

where q_i denotes the percentage of the population in exposure to HI above a certain threshold for demographic group *i*; i.e., non-Hispanic White or adults (age 20–65). Larger values of absolute disparity represent a higher percentage of a certain group under heat risk, suggesting a larger disparity. Positive numbers indicate the analyzed demographic group is more affected by heat risks than the average. In analyzing disparity within regions, we sum up the absolute values for all demographic groups of absolute disparity.

Overall absolute disparity across demographic groups is calculated by

$$\text{Overall absolute disparity} = \left(\sum_i^n |q_i - \mu(q)|\right) \Big/ n. \quad \text{(Equation 4)}$$

Relative disparity by demographic group is calculated as follows:

$$\text{Relative disparity} = \frac{q_i}{\mu(q)} - 1. \quad \text{(Equation 5)}$$

Relative disparity closer to 0 suggests less disparity between a demographic group and the average population. Positive values indicate the demographic group more affected by the heat risk, while negative values indicate the demographic group less affected by the heat risk.

Overall relative disparities across demographic groups are measured by the coefficient of variation (CoV), calculated by

$$\text{CoV} = \frac{\sqrt{\text{Var}(q)}}{\mu(q),} \quad \text{(Equation 6)}$$

where *q* represents the percentage of a population (such as a racial/ethnicity group or age group) exposed to the HI above a certain threshold. In this analysis, the HI thresholds "Caution" and "Extreme Caution" are used.

Population-weighted heat index

We used calculated population-weighted HI in summer months (average HI for June, July, and August for the median values of the outputs from various ESMs) (h_i) in the contiguous US by each sociodemographic group *i* for a given year, as follows:

$$h_i = \frac{\sum_{j=1}^{n} c_j p_{ij}}{\sum_{j=1}^{n} p_{ij},} \quad \text{(Equation 7)}$$

where c_j is the projected average HI for county *j*, and p_{ij} is the projected population of demographic group *i* in county *j*, where a group can be a racial group such as Black population or an age group such as elderly population (age ≥65).

Based on the population-weighted HI, we provide a measure of overall racial/ethnicity disparities considering all counties at the national level as well as between geographic regions (e.g., Northeast, South, Midwest, and South).

RESOURCE AVAILABILITY

Lead contact

Requests for further information and resources should be directed to and will be fulfilled by the lead contact, Angel Hsu (angel.hsu@unc.edu).

Materials availability

This study did not generate new, unique materials.

Data and code availability

Original data have been deposited in the Data-Driven EnviroLab Dataverse public repository at Dataverse: https://doi.org/10.15139/S3/BVAVFU.

ACKNOWLEDGMENTS

A.H. and T.C. were supported by the National Aeronautics and Space Administration grant 80NSSC24K0505. W.P. acknowledges the funding support from Princeton's School of Public and International Affairs. Pacific Northwest National Laboratory is operated for the DOE by Battelle Memorial Institute under contract DE-AC05-76RL01830.

AUTHOR CONTRIBUTIONS

K.S. led data collection, analysis, study design, and writing; A.H. conceptualized the study and supported data analysis and writing; and T.C., W.P., Y.Y., and N.K. provided input on the study design. All authors contributed to the writing of the manuscript.

DECLARATION OF INTERESTS

The authors declare no competing interests.

SUPPLEMENTAL INFORMATION

Supplemental information can be found online at https://doi.org/10.1016/j.oneear.2025.101528.

Received: May 17, 2024
Revised: October 30, 2025
Accepted: November 7, 2025
Published: December 9, 2025

REFERENCES

1. Hsiang, S.M., Burke, M., and Miguel, E. (2013). Quantifying the Influence of Climate on Human Conflict. Science *341*, 1235367. https://doi.org/10.1126/science.1235367.
2. Burke, M., Hsiang, S.M., and Miguel, E. (2015). Global non-linear effect of temperature on economic production. Nature *527*, 235–239. https://doi.org/10.1038/nature15725.
3. Yang, J., Zhou, M., Ren, Z., Li, M., Wang, B., Liu, D.L., Ou, C.-Q., Yin, P., Sun, J., Tong, S., et al. (2021). Projecting heat-related excess mortality under climate change scenarios in China. Nat. Commun. *12*, 1039. https://doi.org/10.1038/s41467-021-21305-1.
4. Fan, Y., Pei-Syuan, L., Im, E.-S., and Lo, M.-H. (2022). Regional disparities in the exposure to heat-related mortality risk under 1.5°C and 2°C global warming. Environ. Res. Lett. *17*, 054009. https://doi.org/10.1088/1748-9326/ac5adf.
5. Ebi, K.L., Capon, A., Berry, P., Broderick, C., de Dear, R., Havenith, G., Honda, Y., Kovats, R.S., Ma, W., Malik, A., et al. (2021). Hot weather and heat extremes: health risks. Lancet *398*, 698–708. https://doi.org/10.1016/S0140-6736(21)01208-3.
6. Wang, J., Chen, Y., Tett, S.F.B., Yan, Z., Zhai, P., Feng, J., and Xia, J. (2020). Anthropogenically-driven increases in the risks of summertime compound hot extremes. Nat. Commun. *11*, 528. https://doi.org/10.1038/s41467-019-14233-8.
7. Wang, J., Chen, Y., Liao, W., He, G., Tett, S.F.B., Yan, Z., Zhai, P., Feng, J., Ma, W., Huang, C., and Hu, Y. (2021). Anthropogenic emissions and urbanization increase risk of compound hot extremes in cities. Nat. Clim. Chang. *11*, 1084–1089. https://doi.org/10.1038/s41558-021-01196-2.
8. Vicedo-Cabrera, A.M., Scovronick, N., Sera, F., Royé, D., Schneider, R., Tobias, A., Astrom, C., Guo, Y., Honda, Y., Hondula, D.M., et al. (2021). The burden of heat-related mortality attributable to recent human-induced climate change. Nat. Clim. Chang. *11*, 492–500. https://doi.org/10.1038/s41558-021-01058-x.
9. Shindell, D., Zhang, Y., Scott, M., Ru, M., Stark, K., and Ebi, K.L. (2020). The Effects of Heat Exposure on Human Mortality Throughout the United States. GeoHealth *4*, e2019GH000234. https://doi.org/10.1029/2019GH000234.
10. Liu, Z., Anderson, B., Yan, K., Dong, W., Liao, H., and Shi, P. (2017). Global and regional changes in exposure to extreme heat and the relative contributions of climate and population change. Sci. Rep. *7*, 43909.
11. Lesk, C., Anderson, W., Rigden, A., Coast, O., Jägermeyr, J., McDermid, S., Davis, K.F., and Konar, M. (2022). Compound heat and moisture extreme impacts on global crop yields under climate change. Nat. Rev. Earth Environ. *3*, 872–889. https://doi.org/10.1038/s43017-022-00368-8.
12. He, C., Zhang, Y., Schneider, A., Chen, R., Zhang, Y., Ma, W., Kinney, P.L., and Kan, H. (2022). The inequality labor loss risk from future urban warming and adaptation strategies. Nat. Commun. *13*, 3847. https://doi.org/10.1038/s41467-022-31145-2.
13. García-León, D., Casanueva, A., Standardi, G., Burgstall, A., Flouris, A.D., and Nybo, L. (2021). Current and projected regional economic impacts of heatwaves in Europe. Nat. Commun. *12*, 5807. https://doi.org/10.1038/s41467-021-26050-z.
14. van Ruijven, B.J., De Cian, E., and Sue Wing, I. (2019). Amplification of future energy demand growth due to climate change. Nat. Commun. *10*, 2762. https://doi.org/10.1038/s41467-019-10399-3.
15. Diffenbaugh, N.S., and Burke, M. (2019). Global warming has increased global economic inequality. Proc. Natl. Acad. Sci. USA *116*, 9808–9813. https://doi.org/10.1073/pnas.1816020116.
16. Benz, S.A., and Burney, J.A. (2021). Widespread Race and Class Disparities in Surface Urban Heat Extremes Across the United States. Earths Future *9*, e2021EF002016. https://doi.org/10.1029/2021EF002016.
17. Chakraborty, T.C., Newman, A.J., Qian, Y., Hsu, A., and Sheriff, G. (2023). Residential segregation and outdoor urban moist heat stress disparities in the United States. One Earth *6*, 738–750. https://doi.org/10.1016/j.oneear.2023.05.016.
18. Hsu, A., Sheriff, G., Chakraborty, T., and Manya, D. (2021). Disproportionate exposure to urban heat island intensity across major US cities. Nat. Commun. *12*, 2721. https://doi.org/10.1038/s41467-021-22799-5.
19. Chakraborty, T., Hsu, A., Manya, D., and Sheriff, G. (2020). A spatially explicit surface urban heat island database for the United States: Characterization, uncertainties, and possible applications. ISPRS J. Photogramm. Remote Sens. *168*, 74–88. https://doi.org/10.1016/j.isprsjprs.2020.07.021.
20. Chakraborty, T., Hsu, A., Manya, D., and Sheriff, G. (2019). Disproportionately higher exposure to urban heat in lower-income neighborhoods: a multi-city perspective. Environ. Res. Lett. *14*, 105003. https://doi.org/10.1088/1748-9326/ab3b99.
21. Hoffman, J.S., Shandas, V., and Pendleton, N. (2020). The Effects of Historical Housing Policies on Resident Exposure to Intra-Urban Heat: A Study of 108 US Urban Areas. Climate *8*, 12. https://doi.org/10.3390/cli8010012.
22. Manware, M., Dubrow, R., Carrión, D., Ma, Y., and Chen, K. (2022). Residential and Race/Ethnicity Disparities in Heat Vulnerability in the United States. GeoHealth *6*, e2022GH000695. https://doi.org/10.1029/2022GH000695.
23. Frölicher, T.L., and Laufkötter, C. (2018). Emerging risks from marine heat waves. Nat. Commun. *9*, 650. https://doi.org/10.1038/s41467-018-03163-6.

24. Zheng, Z., Zhao, L., and Oleson, K.W. (2021). Large model structural uncertainty in global projections of urban heat waves. Nat. Commun. *12*, 3736. https://doi.org/10.1038/s41467-021-24113-9.

25. Coffel, E.D., Horton, R.M., and De Sherbinin, A. (2018). Temperature and humidity based projections of a rapid rise in global heat stress exposure during the 21st century. Environ. Res. Lett. *13*, 014001.

26. Dahl, K., Licker, R., Abatzoglou, J.T., and Declet-Barreto, J. (2019). Increased frequency of and population exposure to extreme heat index days in the United States during the 21st century. Environ. Res. Commun. *1*, 075002.

27. Chen, Y., and Qin, X. (2022). The Impact of Extreme Temperature Shocks on the Health Status of the Elderly in China. Int. J. Environ. Res. Public Health *19*, 15729. https://doi.org/10.3390/ijerph192315729.

28. Lo, Y.T.E., Mitchell, D.M., Gasparrini, A., Vicedo-Cabrera, A.M., Ebi, K.L., Frumhoff, P.C., Millar, R.J., Roberts, W., Sera, F., Sparrow, S., et al. (2019). Increasing mitigation ambition to meet the Paris Agreement's temperature goal avoids substantial heat-related mortality in U.S. cities. Sci. Adv. *5*, eaau4373. https://doi.org/10.1126/sciadv.aau4373.

29. Jones, B., O'Neill, B.C., McDaniel, L., McGinnis, S., Mearns, L.O., and Tebaldi, C. (2015). Future population exposure to US heat extremes. Nat. Clim. Change *5*, 652–655.

30. EPA (2022). Climate Change Indicators: Heat Waves (EPA).

31. Hoover, F.-A., Meerow, S., Grabowski, Z.J., and McPhearson, T. (2021). Environmental justice implications of siting criteria in urban green infrastructure planning. J. Environ. Policy Plan. *23*, 665–682. https://doi.org/10.1080/1523908X.2021.1945916.

32. O'Neill, B.C., Tebaldi, C., van Vuuren, D.P., Eyring, V., Friedlingstein, P., Hurtt, G., Knutti, R., Kriegler, E., Lamarque, J.-F., Lowe, J., et al. (2016). The Scenario Model Intercomparison Project (ScenarioMIP) for CMIP6. Geosci. Model Dev. (GMD) *9*, 3461–3482. https://doi.org/10.5194/gmd-9-3461-2016.

33. Chakraborty, T., Venter, Z.S., Qian, Y., and Lee, X. (2022). Lower Urban Humidity Moderates Outdoor Heat Stress. AGU Adv. *3*, e2022AV000729. https://doi.org/10.1029/2022AV000729.

34. Di Napoli, C., Pappenberger, F., and Cloke, H.L. (2019). Verification of heat stress thresholds for a health-based heat-wave definition. J. Appl. Meteorol. Climatol. *58*, 1177–1194.

35. National Weather Service (2024). NWS HeatRisk (NWS). https://www.weather.gov/media/safety/NWS-HeatRisk-X3-2024.pdf.

36. Meade, R.D., Akerman, A.P., Notley, S.R., McGinn, R., Poirier, P., Gosselin, P., and Kenny, G.P. (2020). Physiological factors characterizing heat-vulnerable older adults: A narrative review. Environ. Int. *144*, 105909. https://doi.org/10.1016/j.envint.2020.105909.

37. Carr, D., Falchetta, G., and Sue Wing, I. (2024). Population Aging and Heat Exposure in the 21st Century: Which U.S. Regions Are at Greatest Risk and Why? Gerontol. *64*, gnad050. https://doi.org/10.1093/geront/gnad050.

38. Chen, K., De Schrijver, E., Sivaraj, S., Sera, F., Scovronick, N., Jiang, L., Roye, D., Lavigne, E., Kyselý, J., Urban, A., et al. (2024). Impact of population aging on future temperature-related mortality at different global warming levels. Nat. Commun. *15*, 1796.

39. IPCC (2021). Summary for policymakers. In Climate Change 2021: The Physical Science Basis. Contribution of Working Group I to the Sixth Assessment Report of the Intergovernmental Panel on Climate Change (IPCC).

40. Berberian, A.G., Gonzalez, D.J.X., and Cushing, L.J. (2022). Racial Disparities in Climate Change-Related Health Effects in the United States. Curr. Environ. Health Rep. *9*, 451–464. https://doi.org/10.1007/s40572-022-00360-w.

41. Hess, J. (2023). Heat and health inequity: acting on determinants of health to promote heat justice. Nat. Rev. Nephrol. *19*, 143–144. https://doi.org/10.1038/s41581-023-00679-z.

42. Schmeltz, M.T., Sembajwe, G., Marcotullio, P.J., Grassman, J.A., Himmelstein, D.U., and Woolhandler, S. (2015). Identifying individual risk factors and documenting the pattern of heat-related illness through analyses of hospitalization and patterns of household cooling. PLoS One *10*, e0118958.

43. EPA (2021). Climate Change Indicators: Heat-Related Deaths (EPA). https://www.epa.gov/climate-indicators/climate-change-indicators-heat-related-deaths.

44. Kenny, G.P., Yardley, J., Brown, C., Sigal, R.J., and Jay, O. (2010). Heat stress in older individuals and patients with common chronic diseases. Can. Med. Assoc. J. *182*, 1053–1060. https://doi.org/10.1503/cmaj.081050.

45. Romitti, Y., Sue Wing, I., Spangler, K.R., and Wellenius, G.A. (2022). Inequality in the availability of residential air conditioning across 115 US metropolitan areas. PNAS Nexus *1*, pgac210. https://doi.org/10.1093/pnasnexus/pgac210.

46. Hsu, A., Chakraborty, T., Thomas, R., Manya, D., Weinfurter, A., Chin, N.J.W., Goyal, N., and Feierman, A. (2020). Measuring What Matters, Where It Matters: A Spatially Explicit Urban Environment and Social Inclusion Index for the Sustainable Development Goals. Front. Sustain. Cities *2*, 556484. https://doi.org/10.3389/frsc.2020.556484.

47. Morello-Frosch, R., and Obasogie, O.K. (2023). The Climate Gap and the Color Line — Racial Health Inequities and Climate Change. N. Engl. J. Med. *388*, 943–949. https://doi.org/10.1056/NEJMsb2213250.

48. Sabrin, S., Zech, W.C., Nazari, R., and Karimi, M. (2021). Understanding occupational heat exposure in the United States and proposing a quantifying stress index. Int. Arch. Occup. Environ. Health *94*, 1983–2000. https://doi.org/10.1007/s00420-021-01711-0.

49. US Bureau of Labor Statistics; US Department of Labor; The Economics Daily (2023). 32.9 Percent of Employees Had Regular Outdoor Exposure in 2022 (BLS). https://www.bls.gov/opub/ted/2023/32-9-percent-of-employees-had-regular-outdoor-exposure-in-2022.htm.

50. The Conference Board (2021). Rates of Remote Work Vary Widely Across US States (TCB). https://www.conference-board.org/publications/remote-work-us.

51. US Bureau of Labor Statistics (2023). Occupational Employment and Wage Statistics (BLS). https://www.bls.gov/oes/notices/2023/occupational-employment-and-wage-statistics-oews.htm.

52. Parsons, L.A., Shindell, D., Tigchelaar, M., Zhang, Y., and Spector, J.T. (2021). Increased labor losses and decreased adaptation potential in a warmer world. Nat. Commun. *12*, 7286. https://doi.org/10.1038/s41467-021-27328-y.

53. Zander, K.K., Botzen, W.J.W., Oppermann, E., Kjellstrom, T., and Garnett, S.T. (2015). Heat stress causes substantial labour productivity loss in Australia. Nat. Clim. Chang. *5*, 647–651. https://doi.org/10.1038/nclimate2623.

54. Malloy, J.T., and Ashcraft, C.M. (2020). A framework for implementing socially just climate adaptation. Clim. Change *160*, 1–14. https://doi.org/10.1007/s10584-020-02705-6.

55. EPA (2023). Inflation Reduction Act Environmental and Climate Justice Program (EPA). https://www.epa.gov/inflation-reduction-act/inflation-reduction-act-environmental-and-climate-justice-program.

56. Oke, T.R. (1995). The heat island of the urban boundary layer: characteristics, causes and effects. In Wind Climate in Cities, J.E. Cermak, A.G. Davenport, E.J. Plate, and D.X. Viegas, eds. (Springer), pp. 81–107. https://doi.org/10.1007/978-94-017-3686-2_5.

57. Kim, S.W., and Brown, R.D. (2021). Urban heat island (UHI) variations within a city boundary: A systematic literature review. Renew. Sustain. Energy Rev. *148*, 111256.

58. Chakraborty, T.C., Qian, Y., Li, J., Leung, L.R., and Sarangi, C. (2025). Daytime urban heat stress in North America reduced by irrigation. Nat. Geosci. *18*, 57–64.

59. Pierce, D.W., Cayan, D.R., Maurer, E.P., Abatzoglou, J.T., and Hegewisch, K.C. (2015). Improved Bias Correction Techniques for Hydrological Simulations of Climate Change. J. Hydrometeorol. *16*, 2421–2442. https://doi.org/10.1175/JHM-D-14-0236.1.

60. Eyring, V., Bony, S., Meehl, G.A., Senior, C.A., Stevens, B., Stouffer, R.J., and Taylor, K.E. (2016). Overview of the Coupled Model Intercomparison

Project Phase 6 (CMIP6) experimental design and organization. Geosci. Model Dev. (GMD) *9*, 1937–1958. https://doi.org/10.5194/gmd-9-1937-2016.

61. Gillingham, K., Nordhaus, W., Anthoff, D., Blanford, G., Bosetti, V., Christensen, P., McJeon, H., and Reilly, J. (2018). Modeling Uncertainty in Integrated Assessment of Climate Change: A Multimodel Comparison. J. Assoc. Environ. Resour. Econ. *5*, 791–826. https://doi.org/10.1086/698910.

62. Lafferty, D.C., and Sriver, R.L. (2023). Downscaling and bias-correction contribute considerable uncertainty to local climate projections in CMIP6. NPJ Clim. Atmos. Sci. *6*, 158. https://doi.org/10.1038/s41612-023-00486-0.

63. Wear, D.N., and Prestemon, J.P. (2019). Spatiotemporal downscaling of global population and income scenarios for the United States. PLoS One *14*, e0219242. https://doi.org/10.1371/journal.pone.0219242.

64. Murakami, D., Yoshida, T., and Yamagata, Y. (2021). Gridded GDP Projections Compatible With the Five SSPs (Shared Socioeconomic Pathways). Front. Built Environ. *7*, 760306. https://doi.org/10.3389/fbuil.2021.760306.

65. Lüthi, S., Fairless, C., Fischer, E.M., Scovronick, N., Ben, A., Coelho, M.D.S.Z.S., Guo, Y.L., Guo, Y., Honda, Y., Huber, V., et al. (2023). Rapid increase in the risk of heat-related mortality. Nat. Commun. *14*, 4894. https://doi.org/10.1038/s41467-023-40599-x.

66. Anderson, G.B., Bell, M.L., and Peng, R.D. (2013). Methods to Calculate the Heat Index as an Exposure Metric in Environmental Health Research. Environ. Health Perspect. *121*, 1111–1119. https://doi.org/10.1289/ehp.1206273.

67. Rothfusz, L.P. (1990). NWS Technical Attachment (SR 90-23).

68. Harper, S., Ruder, E., Roman, H.A., Geggel, A., Nweke, O., Payne-Sturges, D., and Levy, J.I. (2013). Using Inequality Measures to Incorporate Environmental Justice into Regulatory Analyses. Int. J. Environ. Res. Public Health *10*, 4039–4059. https://doi.org/10.3390/ijerph10094039.

69. Jbaily, A., Zhou, X., Liu, J., Lee, T.-H., Kamareddine, L., Verguet, S., and Dominici, F. (2022). Air pollution exposure disparities across US population and income groups. Nature *601*, 228–233. https://doi.org/10.1038/s41586-021-04190-y.

70. Colmer, J., Hardman, I., Shimshack, J., and Voorheis, J. (2020). Disparities in $PM_{2.5}$ air pollution in the United States. Science *369*, 575–578. https://doi.org/10.1126/science.aaz9353.

One Earth, Volume *9*

Supplemental information

Projected widening of sociodemographic heat disparities in the United States by end of century

Kaihui Song, Angel Hsu, TC Chakraborty, Wei Peng, Ying Yu, and Noah Kittner

Supplemental Methods

CMIP6 models

CMIP6 (Coupled Model Intercomparison Project 6): We obtain near-surface air temperature (2m above the ground) (*tas*) and corresponding relative humidity (*hurs*) from ScenarioMIP in CMIP6. This database provides a range of outcomes based on concentration-driven simulations from participating global coupled Earth System Models (ESMs)[1]. ScenarioMIP specifically provides multi-model climate projections based on different scenarios with future emissions and land use changes produced with Integrated Assessment Models (IAMs), using 1995–2014 as the historical baseline for simulations [2]. Figure S1 illustrates the coupled SSP-RCP simulations in CMIP6.

Our analysis focuses on Tier 1 experiments (SSP1-RCP2.6, SSP2-RCP4.5, SSP3-RCP7.0, and SSP5-RCP8.5) and the additional scenario designed to limit global warming to 1.5 degrees Celsius above 1850–1900 (a period often used as a proxy for pre-industrial conditions), SSP1-RCP1.9. A detailed description of these scenarios under focus is provided in Table S1.

Table S1. Coupled Shared Socioeconomic Pathways (SSP) and Representative Concentration Pathways (RCP) scenarios considered in this study

SSP-RCP Pathways	Description
SSP1-RCP1.9	Very low GHG emissions: CO_2 emissions cut to net zero around 2050
SSP1-RCP2.6	Low GHG emissions: CO_2 emissions cut to net zero around 2075
SSP2-RCP4.5	Intermediate GHG emissions: CO_2 emissions around current levels until 2050, then falling but not reaching net zero by 2100
SSP3-RCP7.0	High GHG emissions: CO_2 emissions double by 2100
SSP5-RCP8.5	Very high GHG emissions: CO_2 emissions triple by 2075

We selected 25 models that performed the projection of near-surface air temperature (*tas*) and near-surface relative humidity (*hurs*) to 2100. From these, we identified 4 models for SSP1-RCP1.9, 16 models for SSP1-RCP2.6, 17 models for SSP2-RCP4.5, 16 models for SSP3-RCP7.0, and 17 models for SSP5-RCP8.5 to calculate Heat Index (Table S2).

Table S2. Model details from CMIP6

ID	Models	Model county	Model Institute	Resolution (actual grid resolution specified)	Experiments	Variable		Ensemble variant
						tas	hurs	
1	AWI-CM-1-1-MR	Germany	Alfred Wegener Institute (AWI)	100km	SSP1-RCP1.9	0	0	r1i1p1
					SSP1-RCP2.6	1	1	
					SSP2-RCP4.5	1	1	
					SSP3-RCP7.0	1	1	
					SSP5-RCP8.5	1	1	
2	BCC-CSM2-MR	China	Beijing Climate Center (BCC)	100km (320 x 160 longitude/latitude)	SSP1-RCP1.9	0	0	r1i1p1
					SSP1-RCP2.6	1	0	
					SSP2-RCP4.5	1	0	
					SSP3-RCP7.0	1	0	
					SSP5-RCP8.5	1	0	
3	CAMS-CSM1-0	China	Chinese Academy of Meteorological Sciences (CAMS)	100km (320 x 160 longitude/latitude)	SSP1-RCP1.9	1	0	r1i1p1
					SSP1-RCP2.6	1	0	
					SSP2-RCP4.5	1	0	
					SSP3-RCP7.0	1	0	
					SSP5-RCP8.5	1	0	
4	CAS-ESM2-0	China	Chinese Academy of Sciences (CAS)	100km (256 x 128 longitude/latitude)	SSP1-RCP1.9	0	0	r1i1p1
					SSP1-RCP2.6	1	1	
					SSP2-RCP4.5	1	1	
					SSP3-RCP7.0	1	1	
					SSP5-RCP8.5	1	1	
5	CESM2-WACCM	USA	National Center for Atmospheric Research (NCAR)	100km (0.9x1.25 finite volume grid; 288 x 192 longitude/latitude)	SSP1-RCP1.9	0	0	r1i1p1
					SSP1-RCP2.6	1	1	
					SSP2-RCP4.5	1	1	
					SSP3-RCP7.0	1	1	
					SSP5-RCP8.5	1	1	
6	CIESM	China	Tsinghua University	100km (288 x 192 longitude/latitude)	SSP1-RCP1.9	0	0	r1i1p1
					SSP1-RCP2.6	1	0	
					SSP2-RCP4.5	1	0	
					SSP3-RCP7.0	0	0	
					SSP5-RCP8.5	1	0	
7	CMCC-CM2-SR5	Italy	Fondazione Centro Euro-Mediterraneo sui Cambiamenti Climatici (CMCC)	100km (1deg; 288 x 192 longitude/latitude)	SSP1-RCP1.9	0	0	r1i1p1
					SSP1-RCP2.6	1	1	
					SSP2-RCP4.5	1	1	
					SSP3-RCP7.0	1	1	
					SSP5-RCP8.5	1	1	
8	CMCC-ESM2	Italy	Fondazione Centro Euro-Mediterraneo sui Cambiamenti Climatici (CMCC)	100km (1deg; 288 x 192 longitude/latitude)	SSP1-RCP1.9	0	0	r1i1p1
					SSP1-RCP2.6	1	1	
					SSP2-RCP4.5	1	1	
					SSP3-RCP7.0	1	1	

					SSP5-RCP8.5	1	1	
9	E3SM-1-0	United States	E3SM-Project LLNL UCI UCSB	100km (deg average grid spacing; 90 x 90 x 6 longitude/latitude/cubeface)	SSP1-RCP1.9	0	0	r1i1p1
					SSP1-RCP2.6	0	0	
					SSP2-RCP4.5	0	0	
					SSP3-RCP7.0	0	0	
					SSP5-RCP8.5	1	0	
10	E3SM-1-1	USA	E3SM-Project; RUBISCO	100km (1 deg average grid spacing; 90 x 90 x 6 longitude/latitude/cubeface)	SSP1-RCP1.9	0	0	r1i1p1
					SSP1-RCP2.6	0	0	
					SSP2-RCP4.5	1	0	
					SSP3-RCP7.0	0	0	
					SSP5-RCP8.5	1	0	
11	E3SM-1-1-ECA	United States	E3SM-Project	100km (90 x 90 x 6 longitude/latitude/cubeface)	SSP1-RCP1.9	0	0	r1i1p1
					SSP1-RCP2.6	0	0	
					SSP2-RCP4.5	0	0	
					SSP3-RCP7.0	0	0	
					SSP5-RCP8.5	1	0	
12	EC-Earth3	Spain, Italy, Germany, UK, Finland, Switzerland	EC-Earth-Consortium	100km (linearly reduced Gaussian grid equivalent to 512 x 256 longitude/latitude)	SSP1-RCP1.9	0	0	r1i1p1
					SSP1-RCP2.6	1	1	
					SSP2-RCP4.5	1	1	
					SSP3-RCP7.0	1	1	
					SSP5-RCP8.5	1	1	
13	EC-Earth3-CC	Spain, Italy, Germany, UK, Finland, Switzerland	EC-Earth-Consortium	100km (linearly reduced Gaussian grid equivalent to 512 x 256 longitude/latitude)	SSP1-RCP1.9	0	0	r1i1p1
					SSP1-RCP2.6	0	0	
					SSP2-RCP4.5	1	1	
					SSP3-RCP7.0	0	0	
					SSP5-RCP8.5	1	1	
14	EC-Earth3-AerChem	Spain, Italy, Germany, UK, Finland, Switzerland	EC-Earth-Consortium	100km (linearly reduced Gaussian grid equivalent to 512 x 256 longitude/latitude)	SSP1-RCP1.9	0	0	r1i1p1
					SSP1-RCP2.6	0	0	
					SSP2-RCP4.5	0	0	
					SSP3-RCP7.0	1	1	
					SSP5-RCP8.5	0	0	
15	EC-Earth3-Veg	Spain, Italy, Germany, UK, Finland, Switzerland	EC-Earth-Consortium	100km (linearly reduced Gaussian grid equivalent to 512 x 256 longitude/latitude)	SSP1-RCP1.9	1	1	r1i1p1
					SSP1-RCP2.6	1	1	
					SSP2-RCP4.5	1	1	
					SSP3-RCP7.0	1	1	
					SSP5-RCP8.5	1	1	
16	EC-Earth3-Veg-LR	Spain, Italy, Germany, UK, Finland, Switzerland	EC-Earth-Consortium	100km (linearly reduced Gaussian grid equivalent to 512 x 256 longitude/latitude)	SSP1-RCP1.9	1	1	r1i1p1
					SSP1-RCP2.6	1	1	
					SSP2-RCP4.5	1	1	
					SSP3-RCP7.0	1	1	
					SSP5-RCP8.5	1	1	
17	FGOALS-f3-L	China	Chinese Academy of Sciences (CAS)	100km (360 x 180 longitude/latitude)	SSP1-RCP1.9	0	0	r1i1p1
					SSP1-RCP2.6	1	1	

					SSP2-RCP4.5	1	1	
					SSP3-RCP7.0	1	1	
					SSP5-RCP8.5	1	1	
18	FIO-ESM-2-0	China	First Institute of Oceanography, Qingdao National Laboratory for Marine Science and Technology (FIO-QLNM)	100 km (0.9x1.25 finite volume grid; 192 x 288 longitude/latitude)	SSP1-RCP1.9	0	0	r1i1p1
					SSP1-RCP2.6	1	1	
					SSP2-RCP4.5	1	1	
					SSP3-RCP7.0	0	0	
					SSP5-RCP8.5	1	1	
19	GFDL-ESM4	USA	National Oceanic and Atmospheric Administration, Geophysical Fluid Dynamics Laboratory (NOAA-GFDL)	100km (1 degree nominal horizontal resolution; 360 x 180 longitude/latitude)	SSP1-RCP1.9	1	1	r1i1p1
					SSP1-RCP2.6	1	1	
					SSP2-RCP4.5	1	1	
					SSP3-RCP7.0	1	1	
					SSP5-RCP8.5	1	1	
20	INM-CM4-8	Russia	Institute for Numerical Mathematics (INM)	100km (2x1.5; 180 x 120 longitude/latitude; 21 levels; top level sigma = 0.01))	SSP1-RCP1.9	0	0	r1i1p1
					SSP1-RCP2.6	1	1	
					SSP2-RCP4.5	1	1	
					SSP3-RCP7.0	1	1	
					SSP5-RCP8.5	1	1	
21	INM-CM5-0	Russia	Institute for Numerical Mathematics (INM)	100km (2x1.5; 180 x 120 longitude/latitude; 73 levels; top level sigma = 0.0002)	SSP1-RCP1.9	0	0	r1i1p1
					SSP1-RCP2.6	1	1	
					SSP2-RCP4.5	1	1	
					SSP3-RCP7.0	1	1	
					SSP5-RCP8.5	1	1	
22	MPI-ESM1-2-HR	Germany	Max Planck Institute for Meteorology (MPI-M); Deutscher Wetterdienst (DWD); Deutsches Klimarechenzentrum (DKRZ)	100km (spectral T127; 384 x 192 longitude/latitude; 95 levels; top level 0.01 hPa)	SSP1-RCP1.9	0	0	r1i1p1
					SSP1-RCP2.6	1	1	
					SSP2-RCP4.5	1	1	
					SSP3-RCP7.0	1	1	
					SSP5-RCP8.5	1	1	
23	MRI-ESM2-0	Japan	Meteorological Research Institute (MRI)	100km (320 x 160 longitude/latitude; 80 levels; top level 0.01 hPa)	SSP1-RCP1.9	1	1	r1i1p1
					SSP1-RCP2.6	1	1	
					SSP2-RCP4.5	1	1	
					SSP3-RCP7.0	1	1	
					SSP5-RCP8.5	1	1	
24	TaiESM1	Taiwan	Research Center for Environmental Changes, Academia Sinica (AS-RCEC)	100km (0.9x1.25 degree; 288 x 192 longitude/latitude; 30 levels; top level ~2 hPa)	SSP1-RCP1.9	0	0	r1i1p1
					SSP1-RCP2.6	1	0	
					SSP2-RCP4.5	1	0	
					SSP3-RCP7.0	1	0	
					SSP5-RCP8.5	1	0	
25	NorESM2-MM	Norway	Norwegian Climate Centre (NCC)	100km (1 degree resolution; 288 x 192; 32 levels; top level 3 mb)	SSP1-RCP1.9	0	0	r1i1p1
					SSP1-RCP2.6	1	1	
					SSP2-RCP4.5	1	1	
					SSP3-RCP7.0	1	1	

					SSP5-RCP8.5	1	1	

Note: "tas" denotes near-surface air temperature (2m above the ground), "hurs" denotes relative humidity. 1 indicates available data; 0 indicates data that is not available. Data sources: https://github.com/WCRP-CMIP/CMIP6_CVs/blob/master/README.m

In the analysis, we used the Heat Index, which is an indicator adopted by the National Weather Service (NWS), to measure how hot it "feels" to the human body. This index is primarily dependent on temperature and humidity, although other factors such as direct sunlight, wind speed, and cloud cover also affect people's perception of heat[3]. We used the median value of near-surface air temperature and near-surface relative humidity for ensemble models to calculate the Heat Index without the bias correction procedures. Some bias correction procedures, such as quantile mapping, are commonly used when analyzing climate impacts, typically with extreme values, at high spatial resolution, such as daily[4,5]. Prior studies suggest that the bias correction process does not systematically over- or under-estimate projected changes in the Heat Index due to the compensatory effect brought by temperature and humidity biases[6].

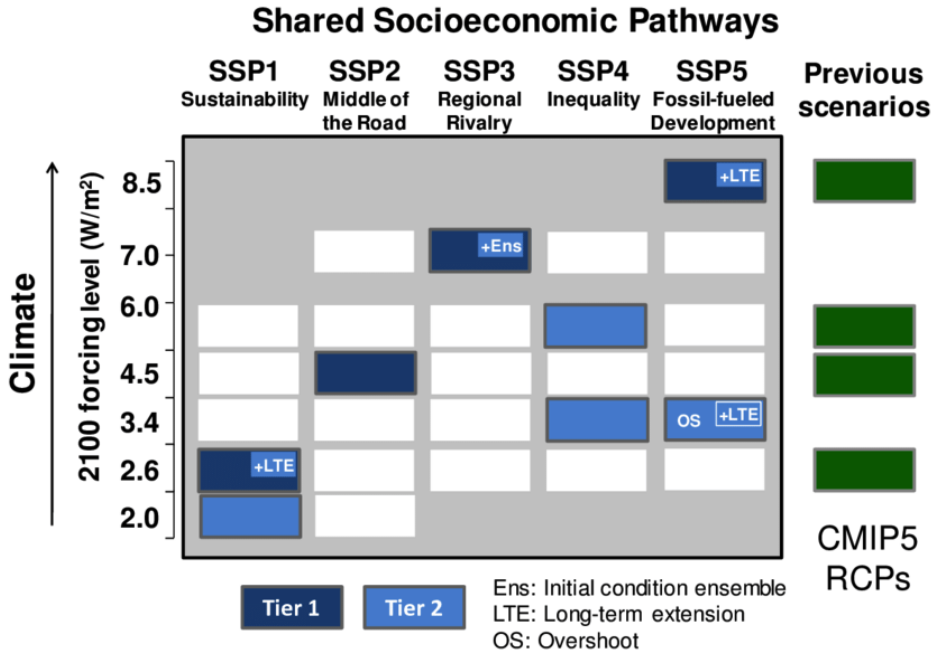

Figure S1 SSP-RCP scenario matrix illustrating ScenarioMIP simulations in CMIP6 [2]

Socioeconomic data

Total population, population by race, age, and gender are county-level projections under five SSPs at a five-year interval from 2020 to 2100[7]. Sociodemographic data collected from multiple sources are detailed in Table S3. In our analysis, populations by race are categorized into *non-Hispanic White*, *non-Hispanic Black*, *Hispanic (all races)*, and *non-Hispanic Other Races*. The age groups under study are classified into *Young (age below 20)*, *Adult (age 20–64)*, and *Elderly (age 65+)*. To get the downscaled data, Hauer[8] calculates cohort-change ratios (CCRs) and cohort-change differences and projects into Leslie matrix population projection models using inputs from autoregressive integrated moving average (ARIMA) models and controls the projections to the SSPs.

Table S3. Downscaled Sociodemographic data and their sources

Socioeconomic factors	Data source	Original spatial resolution	Reference
Urban fraction	Gao et al. (2021)	1/8 degree	[7]
Population	Socioeconomic Data and Applications Center (SEDAC)	US county	[8]
Gender	Socioeconomic Data and Applications Center (SEDAC)	US county	[8]
Race	Socioeconomic Data and Applications Center (SEDAC)	US county	[8]
Age	Socioeconomic Data and Applications Center (SEDAC)	US county	[8]
Income	Murakami	1/12 degree	[9]

Table S4. Probability of having heat disorders with prolonged exposure (summer average HI>80F) under SSP5-RCP8.5

Month	2020	2050	2100	Increase in likelihood of heat disorders (2020–-2050)	Increase in likelihood of heat disorders (2020–-2100)
Jan	0.00	0.00	0.04	0.00	0.04
Feb	0.00	0.00	0.04	0.00	0.04
Mar	0.00	0.01	0.12	0.01	0.12
Apr	0.04	0.10	0.22	0.05	0.18
May	0.19	0.27	0.44	0.08	0.26
Jun	0.35	0.45	0.63	0.10	0.28
Jul	0.47	0.56	0.75	0.09	0.28
Aug	0.47	0.57	0.75	0.10	0.28
Sep	0.32	0.41	0.63	0.09	0.31
Oct	0.17	0.24	0.42	0.07	0.25
Nov	0.04	0.10	0.24	0.06	0.20
Dec	0.00	0.00	0.12	0.00	0.12

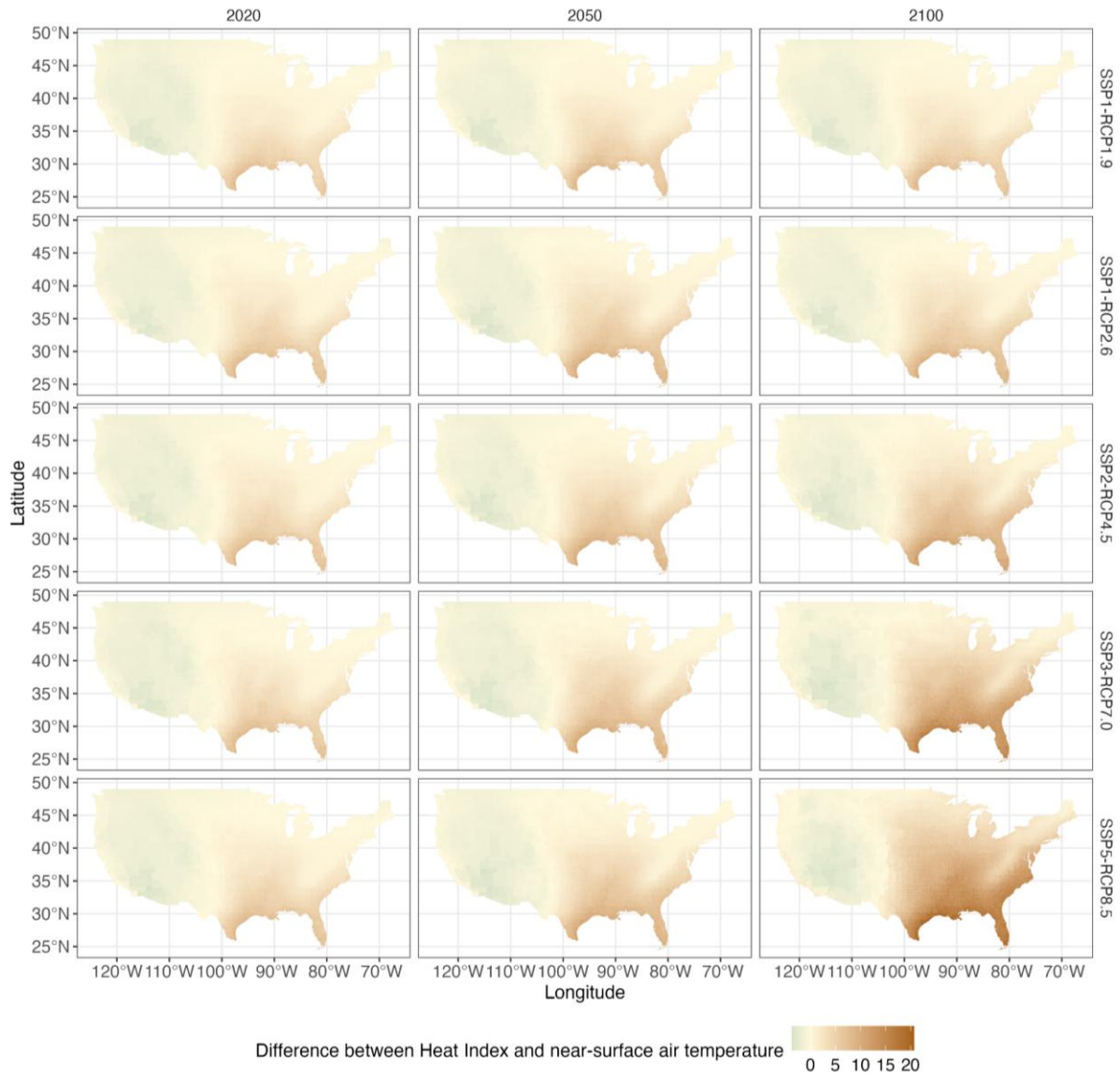

Figure S2 Difference between Heat Index and near-surface air temperature in contiguous US under five coupled SSP-RCP scenarios

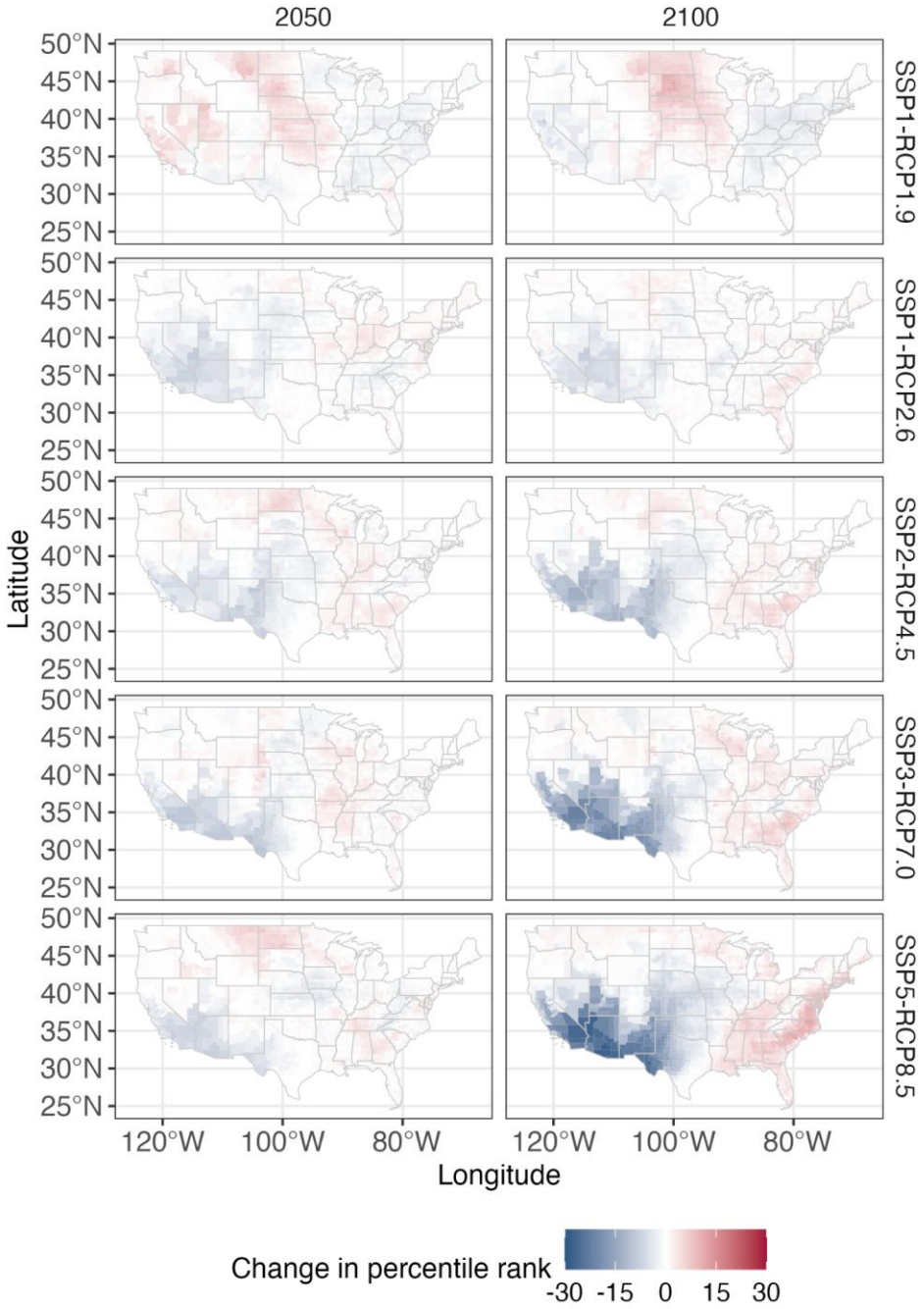

Figure S3 Changes in percentile rank of HI between baseline year (average across 2016 and 2020) and middle of the century (average across 2046 and 2050) (left panel) and between baseline year and the end of the century (average across 2096 and 2100)

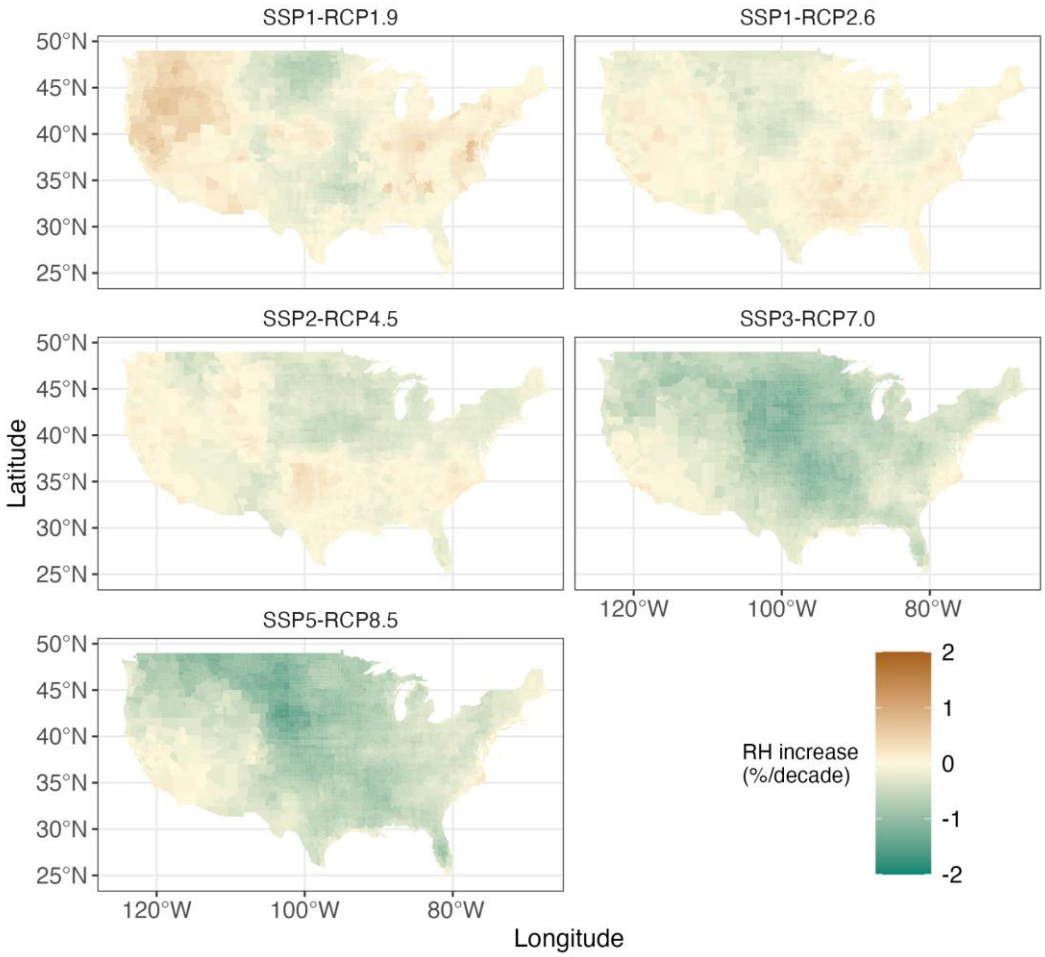

Figure S4 Changes in relative humidity in counties in the contiguous US under five coupled SSP-RCP scenarios

Table S5 Number of counties by Heat Index zones under five coupled SSP-RCP scenarios

Time	SSP-RCP	Region	Safe	Caution	Extreme Caution	Danger
2020	SSP1-RCP1.9	Midwest	1010	45	0	0
		South	578	758	86	0
		West	397	17	0	0
		Northeast	217	0	0	0
		Total	2202	820	86	0
	SSP1-RCP2.6	Midwest	747	308	0	0
		South	479	733	210	0
		West	395	19	0	0
		Northeast	217	0	0	0
		Total	1838	1060	210	0
	SSP2-RCP4.5	Midwest	727	328	0	0
		South	502	710	210	0
		West	390	24	0	0
		Northeast	217	0	0	0
		Total	1836	1062	210	0
	SSP3-RCP7.0	Midwest	769	286	0	0
		South	482	733	207	0
		West	394	20	0	0
		Northeast	217	0	0	0
		Total	1862	1039	207	0
	SSP5-RCP8.5	Midwest	689	366	0	0
		South	429	771	222	0
		West	395	19	0	0

		Northeast	217	0	0	0
		Total	1730	1156	222	0
2050	SSP1-RCP1.9	Midwest	910	145	0	0
		South	531	669	222	0
		West	392	21	1	0
		Northeast	217	0	0	0
		Total	2050	835	223	0
	SSP1-RCP2.6	Midwest	591	464	0	0
		South	345	697	380	0
		West	384	29	1	0
		Northeast	217	0	0	0
		Total	1537	1190	381	0
	SSP2-RCP4.5	Midwest	528	523	4	0
		South	293	686	443	0
		West	381	32	1	0
		Northeast	217	0	0	0
		Total	1419	1241	448	0
	SSP3-RCP7.0	Midwest	534	513	8	0
		Northeast	216	1	0	0
		South	246	645	531	0
		West	380	33	1	0
		Total	1376	1192	540	0
	SSP5-RCP8.5	Midwest	451	584	20	0
		Northeast	215	2	0	0
		South	209	624	589	0

		West	375	37	2	0
		Total	1250	1247	611	0
2100	SSP1-RCP1.9	Midwest	915	140	0	0
		South	534	759	129	0
		West	393	21	0	0
		Northeast	217	0	0	0
		Total	2059	920	129	0
	SSP1-RCP2.6	Midwest	596	459	0	0
		South	321	726	375	0
		West	385	28	1	0
		Northeast	217	0	0	0
		Total	1519	1213	376	0
	SSP2-RCP4.5	Midwest	324	644	87	0
		Northeast	204	13	0	0
		South	145	566	711	0
		West	366	44	4	0
		Total	1039	1267	802	0
	SSP3-RCP7.0	Midwest	81	603	371	0
		Northeast	121	96	0	0
		South	1	365	851	205
		West	285	120	9	0
		Total	488	1184	1231	205
	SSP5-RCP8.5	Midwest	7	372	673	3
		Northeast	33	163	21	0
		South	0	141	670	611

	West	203	193	18	0
	Total	243	869	1382	614

Table S6 Changes in heat exposure between Heat Index zones in 2050 and 2100

Coupled SSP-RCP scenarios	2050			2100					
	No movement (%)	Safe to Caution (%)	Caution to Extreme Caution (%)	No movement (%)	Safe to Caution (%)	Safe to Extreme Caution (%)	Caution to Extreme Caution (%)	Caution to Danger (%)	Extreme Caution to Danger (%)
SSP1-RCP1.9	91.4 (90.7)	2.3 (4.9)	6.2 (4.4)	94.9 (94.0)	2.1 (4.6)	NA	2.9 (1.4)	NA	NA
SSP1-RCP2.6	87.4 (84.8)	6.1 (9.7)	6.5 (5.5)	86.0 (84.4)	6.8 (10.3)	NA	7.2 (5.3)	NA	NA
SSP2-RCP4.5	81.2 (78.9)	10.3 (13.4)	8.5 (7.7)	59.0 (55.3)	26.2 (25.6)	NA	14.9 (19.0)	NA	NA
SSP3-RCP7.0	78.8 (73.6)	11.0 (15.6)	10.2 (10.7)	17.4 (17.0)	45.7 (37.6)	4.3 (6.6)	22 (32.2)	1.8 (0.8)	8.9 (5.8)
SSP5-RCP8.5	72.7 (72.0)	14.9 (15.4)	12.4 (12.5)	7.2 (8.0)	35.5 (27.8)	21.4 (20.0)	15.1 (24.4)	11.2 (12.6)	9.6 (7.1)

Note: the numbers show the percentage of population (numbers out of parentheses) and number of counties (numbers in parentheses) using 2020 as a reference, the percentage may not add up to 100% due to rounding.

Table S7. US Census Regions in the contiguous United States

State	State Code	Region
Alabama	AL	South
Arkansas	AR	South
Arizona	AZ	West
California	CA	West
Colorado	CO	West
Connecticut	CT	Northeast
District of Columbia	DC	South
Delaware	DE	South
Florida	FL	South
Georgia	GA	South
Iowa	IA	Midwest
Idaho	ID	West
Illinois	IL	Midwest
Indiana	IN	Midwest
Kansas	KS	Midwest
Kentucky	KY	South
Louisiana	LA	South
Massachusetts	MA	Northeast
Maryland	MD	South
Maine	ME	Northeast
Michigan	MI	Midwest
Minnesota	MN	Midwest
Missouri	MO	Midwest
Mississippi	MS	South
Montana	MT	West
North Carolina	NC	South
North Dakota	ND	Midwest
Nebraska	NE	Midwest
New Hampshire	NH	Northeast
New Jersey	NJ	Northeast
New Mexico	NM	West
Nevada	NV	West
New York	NY	Northeast
Ohio	OH	Midwest
Oklahoma	OK	South
Oregon	OR	West
Pennsylvania	PA	Northeast
Rhode Island	RI	Northeast
South Carolina	SC	South
South Dakota	SD	Midwest
Tennessee	TN	South
Texas	TX	South
Utah	UT	West
Virginia	VA	South
Vermont	VT	Northeast
Washington	WA	West
Wisconsin	WI	Midwest

West Virginia	WV	South
Wyoming	WY	West

Table S8. Population-weighted Heat Index by race under four coupled SSP-RCP scenarios

Race/Ethnicity	SSP-RCP scenarios	2020	2050	2100
Non-Hispanic White	SSP1-RCP2.6	77.0	79.6	80.3
Non-Hispanic Black	SSP1-RCP2.6	80.0	82.5	82.7
Hispanic (all races)	SSP1-RCP2.6	80.2	82.6	82.7
Non-Hispanic other races	SSP1-RCP2.6	76.5	78.7	79.0
Non-Hispanic White	SSP2-RCP4.5	77.1	80.1	83.7
Non-Hispanic Black	SSP2-RCP4.5	79.9	83.1	86.4
Hispanic (all races)	SSP2-RCP4.5	80.2	83.0	86.0
Non-Hispanic other races	SSP2-RCP4.5	76.5	79.1	82.0
Non-Hispanic White	SSP5-RCP8.5	77.4	81.4	93.3
Non-Hispanic Black	SSP5-RCP8.5	80.4	84.5	96.8
Hispanic (all races)	SSP5-RCP8.5	80.4	84.1	95.3
Non-Hispanic other races	SSP5-RCP8.5	76.7	80.2	91.0
Non-Hispanic White	SSP3-RCP7.0	76.8	80.6	88.7
Non-Hispanic Black	SSP3-RCP7.0	79.8	83.7	91.8
Hispanic (all races)	SSP3-RCP7.0	80.1	83.5	91.0
Non-Hispanic other races	SSP3-RCP7.0	76.3	79.4	86.6

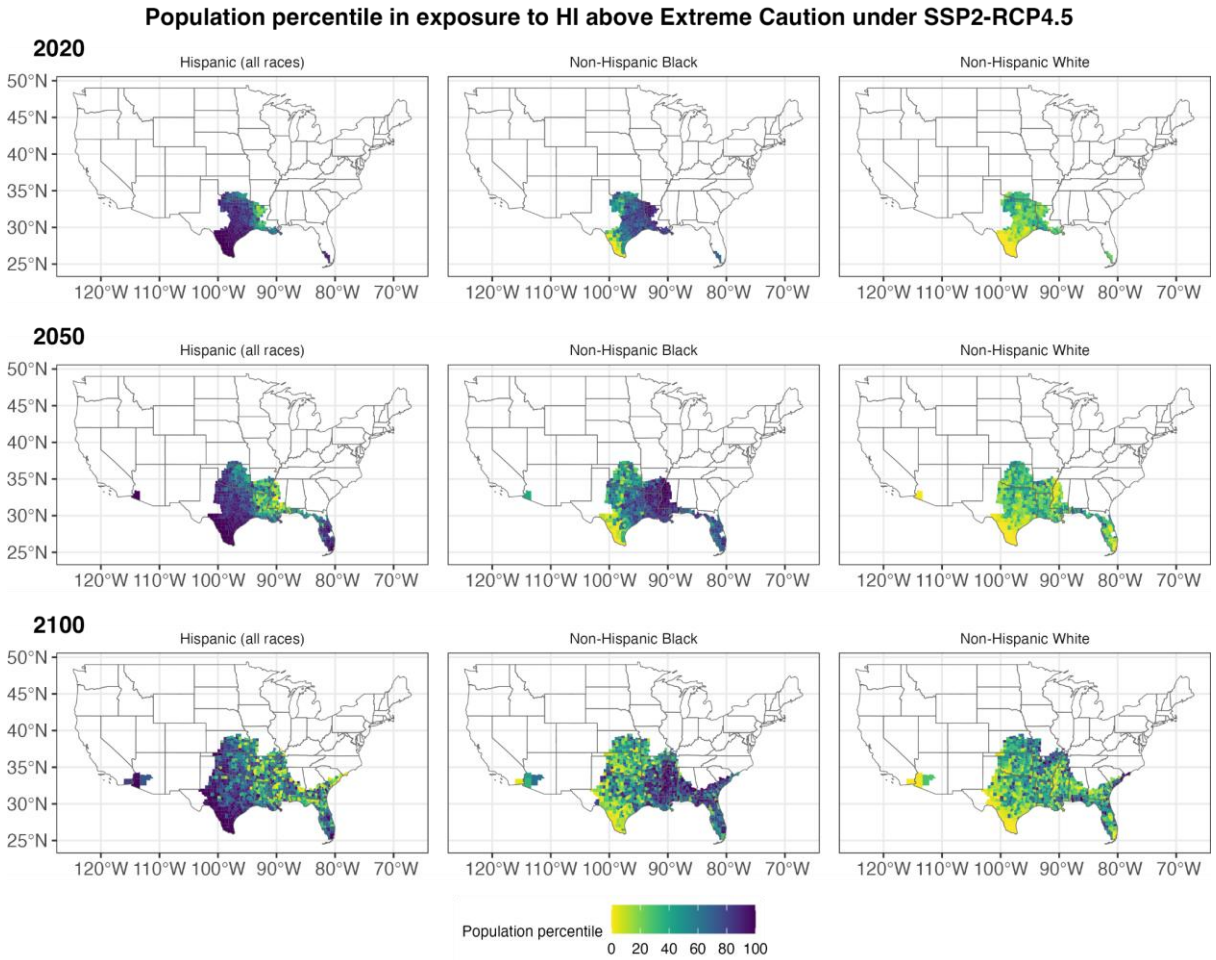

Figure S5 Population percentile of racial/ethnic groups in exposure to HI above Extreme Caution under SSP2-RCP4.5 scenario

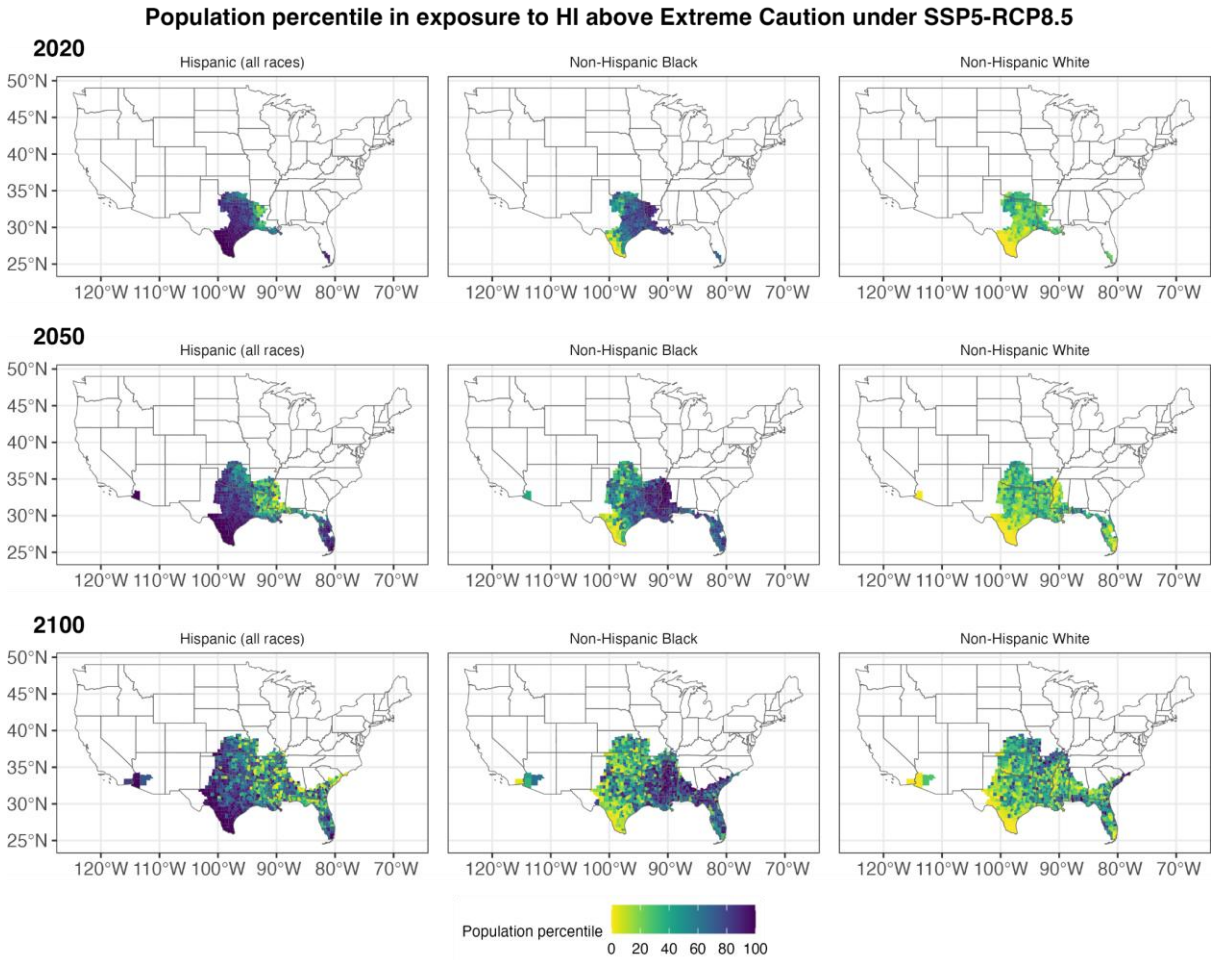

Figure S6 Population percentile of racial/ethnic groups in exposure to HI above Extreme Caution under SSP5-RCP8.5 scenario

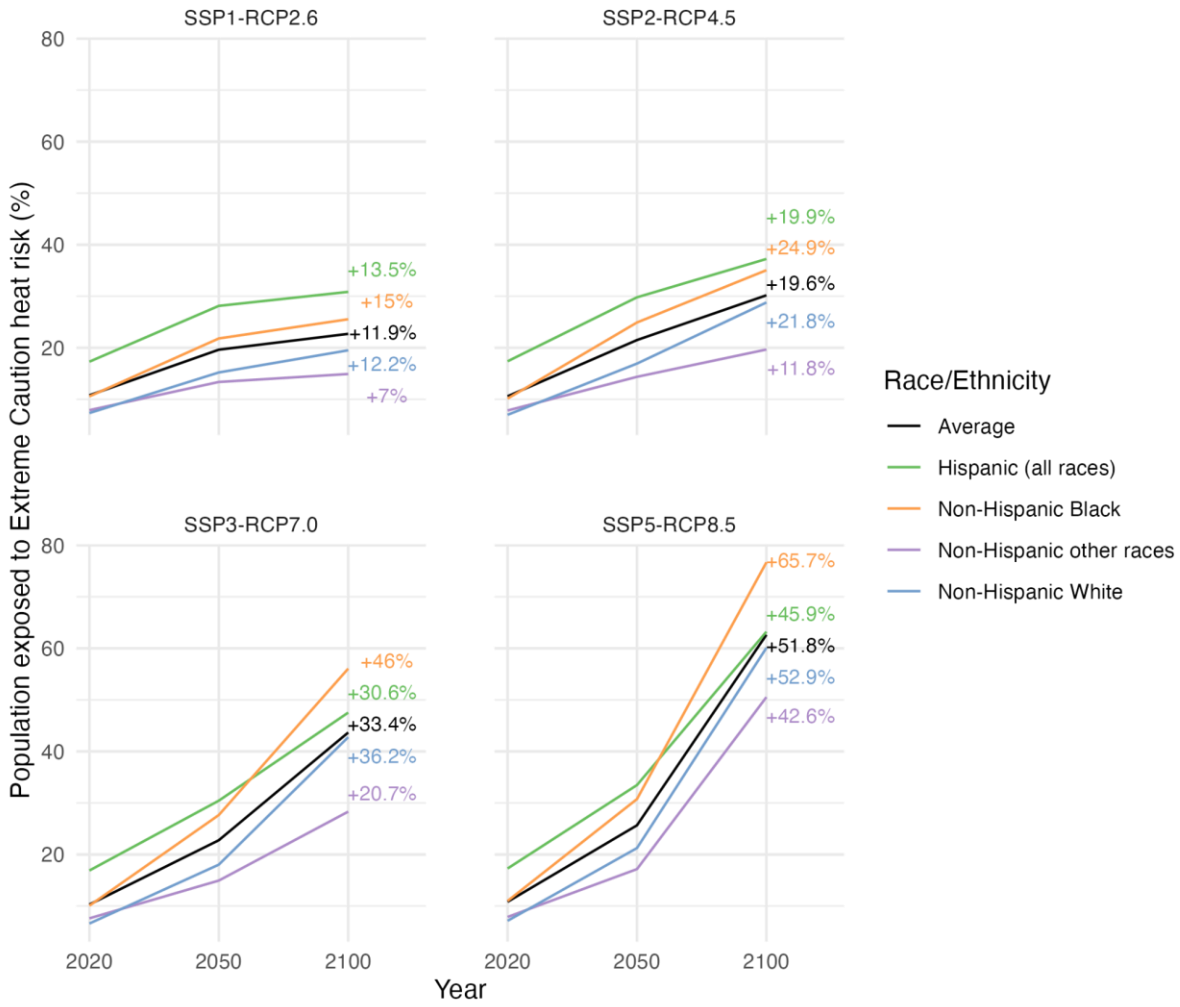

Figure S7 Percentage of population exposed to Extreme Caution+ heat risk under coupled SSP-RCP scenarios by racial/ethnic group

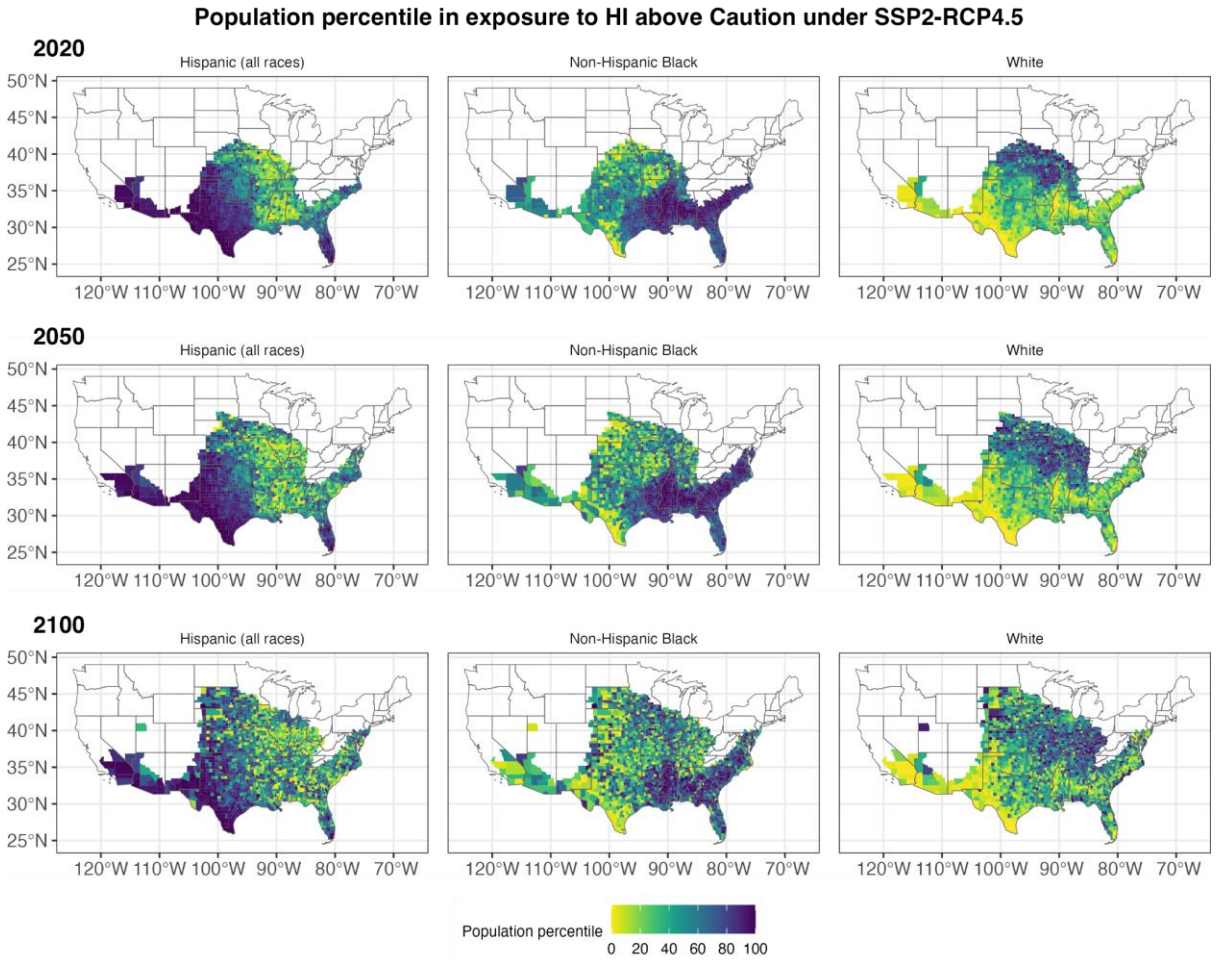

Figure S8 Population percentile of racial/ethnic groups in exposure to HI above Caution under SSP2-RCP4.5 scenario

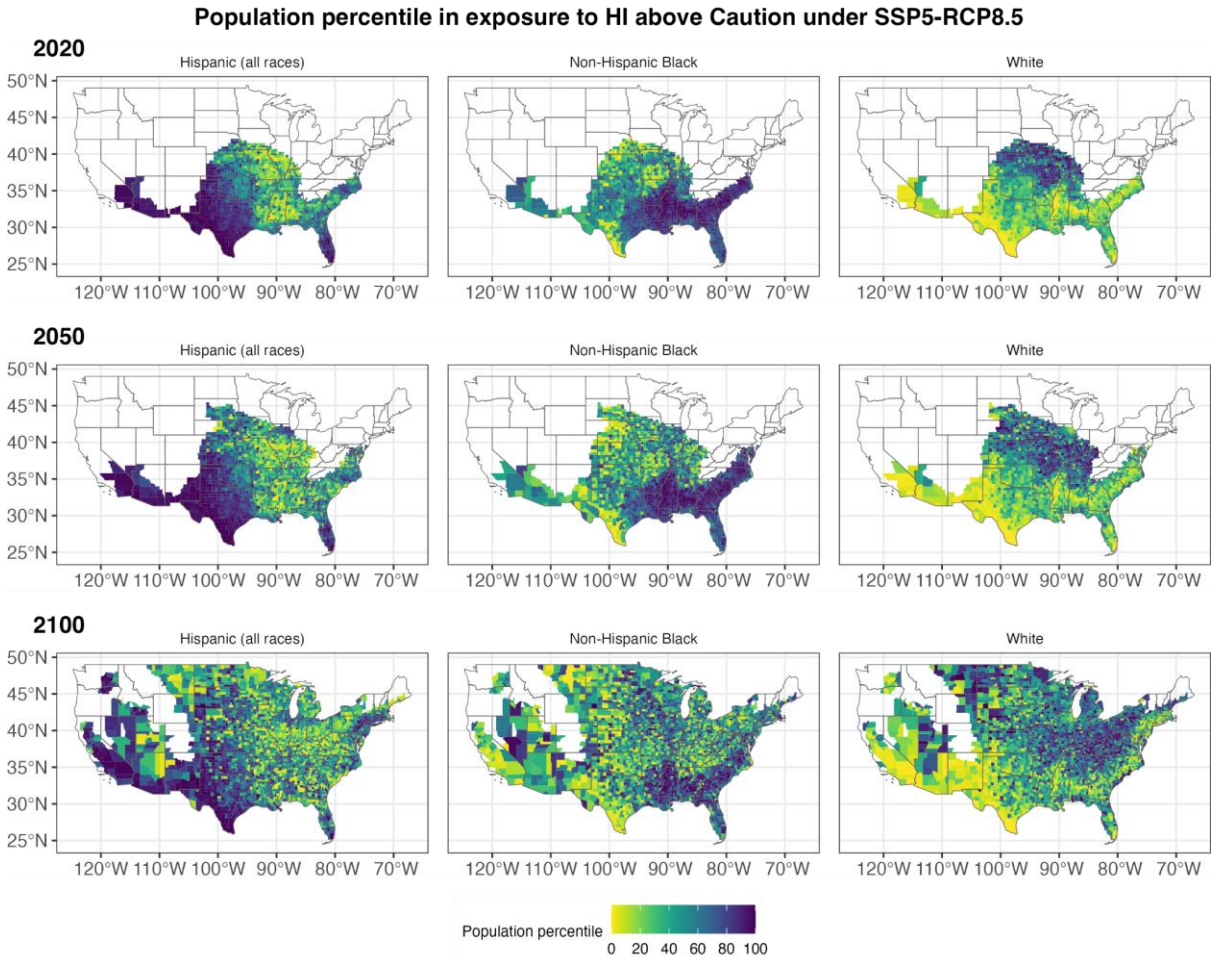

Figure S9 Population percentile of racial/ethnic groups in exposure to HI above Caution under SSP5-RCP8.5 scenario

.

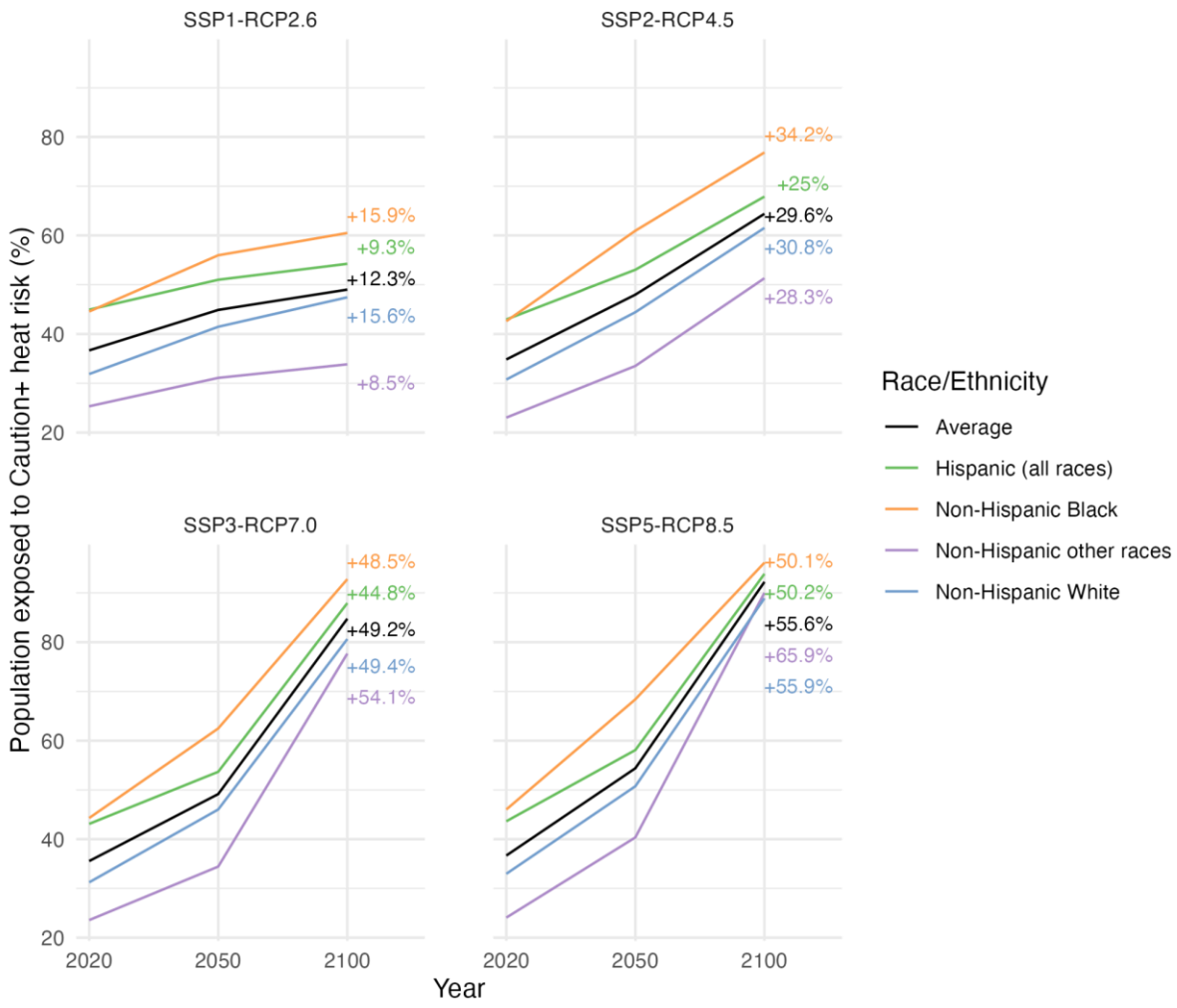

Figure S10 Percentage of population exposed to *Caution* heat risk and above under coupled SSP-RCP scenarios by racial/ethnic group

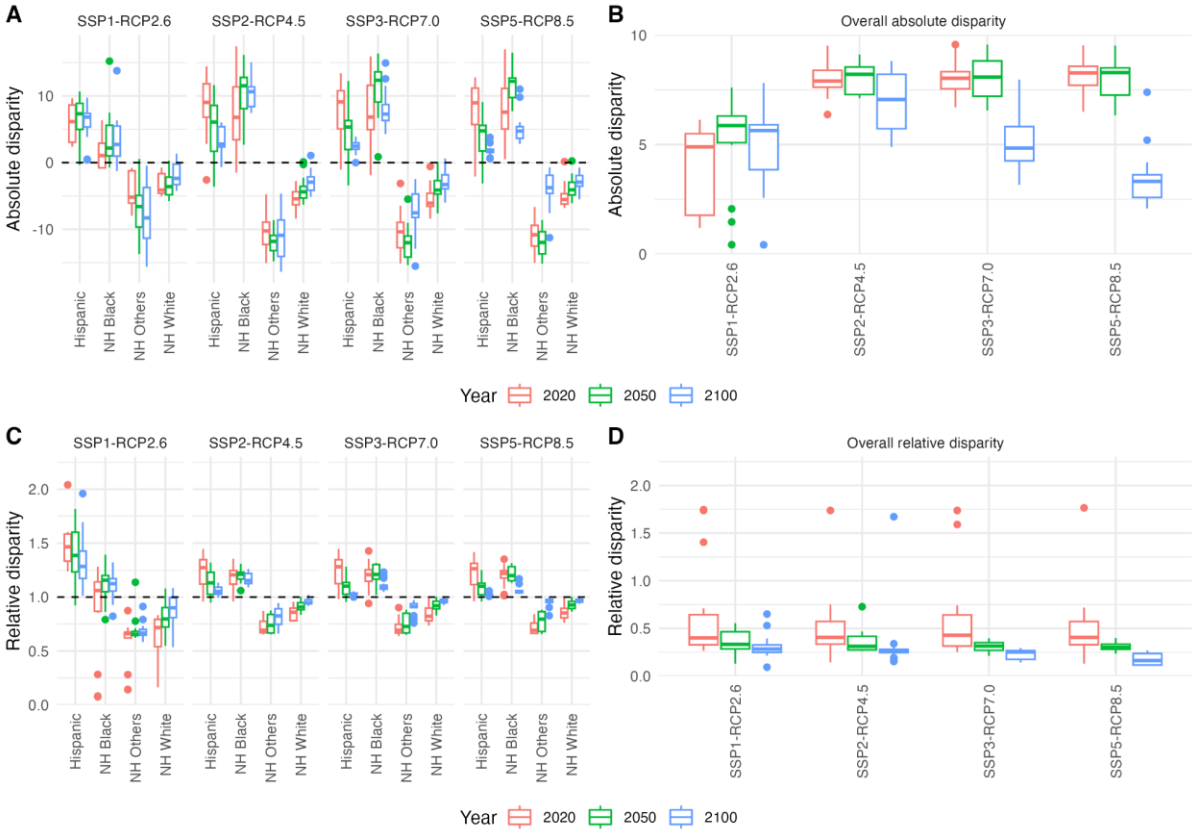

Figure S11 Racial/ethnicity disparity in exposure to Heat Index above *Caution (HI* ≥ 80°*F*) threshold under future scenarios. (A) Absolute disparity of racial-ethnicity groups in exposure to Heat Index above *Caution* threshold under future scenarios; **(B)** Overall absolute disparity in exposure to Heat Index above *Caution* threshold under future scenarios; **(C)** Relative disparity of racial-ethnicity groups in exposure to Heat Index above *Caution* threshold under future scenarios. **(D)** Overall relative disparity of racial-ethnicity groups in exposure to Heat Index above *Caution* threshold under future scenarios; **(**Absolute disparity is measured as the difference between a group's exposure and the overall population average, while relative disparity represents the ratio of a group's exposure to the population average. Hispanic: Hispanic (all races), NH-Black: Non-Hispanic Black, NH-White: Non-Hispanic White, NH-Others: Non-Hispanic Other Races. Each box plot shows the interquartile range (25th–75th percentile), with the median indicated by a horizontal line. Whiskers extend to 1.5× the IQR, and points beyond the whiskers are plotted as outliers. Please see Supplementary Information SI1.1 for more details on the number of models. The black dash lines represent benchmark values for perfect equalization.)

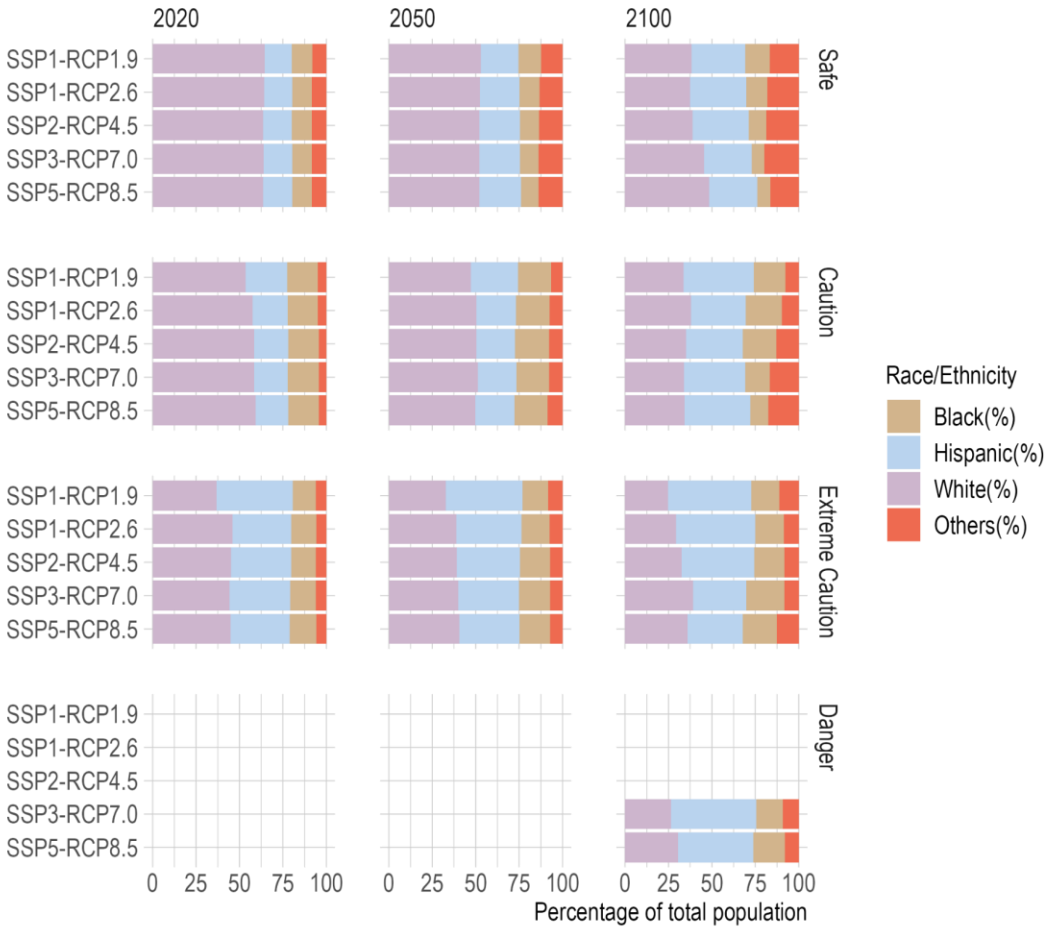

Figure S12 Race/ethnicity composition for each Heat Index zone

Table S9. Percentage of the distribution of non-Hispanic black populations in the bottom and top quartiles of summer Heat Index distributions from 2020 to 2100.

	2020		2050		2100	
	bottom	top	bottom	top	bottom	top
SSP1-RCP1.9	1.67%	3.48%	4.38%	12.5%	5.15%	1.29%
SSP1-RCP2.6	2.19%	12.5%	6.18%	20.36%	13.26%	13.14%
SSP2-RCP4.5	2.45%	11.21%	6.95%	27.06%	22.39%	36.60%
SSP3-RCP7.0	2.45%	11.73%	7.59%	31.83%	41.18%	63.92%
SSP5-RCP8.5	2.45%	13.14%	9.52%	38.53%	57.27%	78.22%

S 2.3.2 Age disparity

Table S10 Population-weighted Heat Index by age under four coupled SSP-RCP scenarios

Age	SSP-RCP scenarios	2020	2050	2100
Adult	SSP1-RCP2.6	77.97	80.63	81.20
Elderly	SSP1-RCP2.6	77.75	80.67	81.45
Young	SSP1-RCP2.6	78.23	80.87	81.32
Adult	SSP2-RCP4.5	77.97	81.12	84.61
Elderly	SSP2-RCP4.5	77.74	81.15	84.82
Young	SSP2-RCP4.5	78.24	81.38	84.76
Adult	SSP3-RCP7.0	77.78	81.59	89.58
Elderly	SSP3-RCP7.0	77.54	81.62	89.78
Young	SSP3-RCP7.0	78.04	81.85	89.74
Adult	SSP5-RCP8.5	78.28	82.34	94.14
Elderly	SSP5-RCP8.5	78.06	82.37	94.32
Young	SSP5-RCP8.5	78.55	82.60	94.31

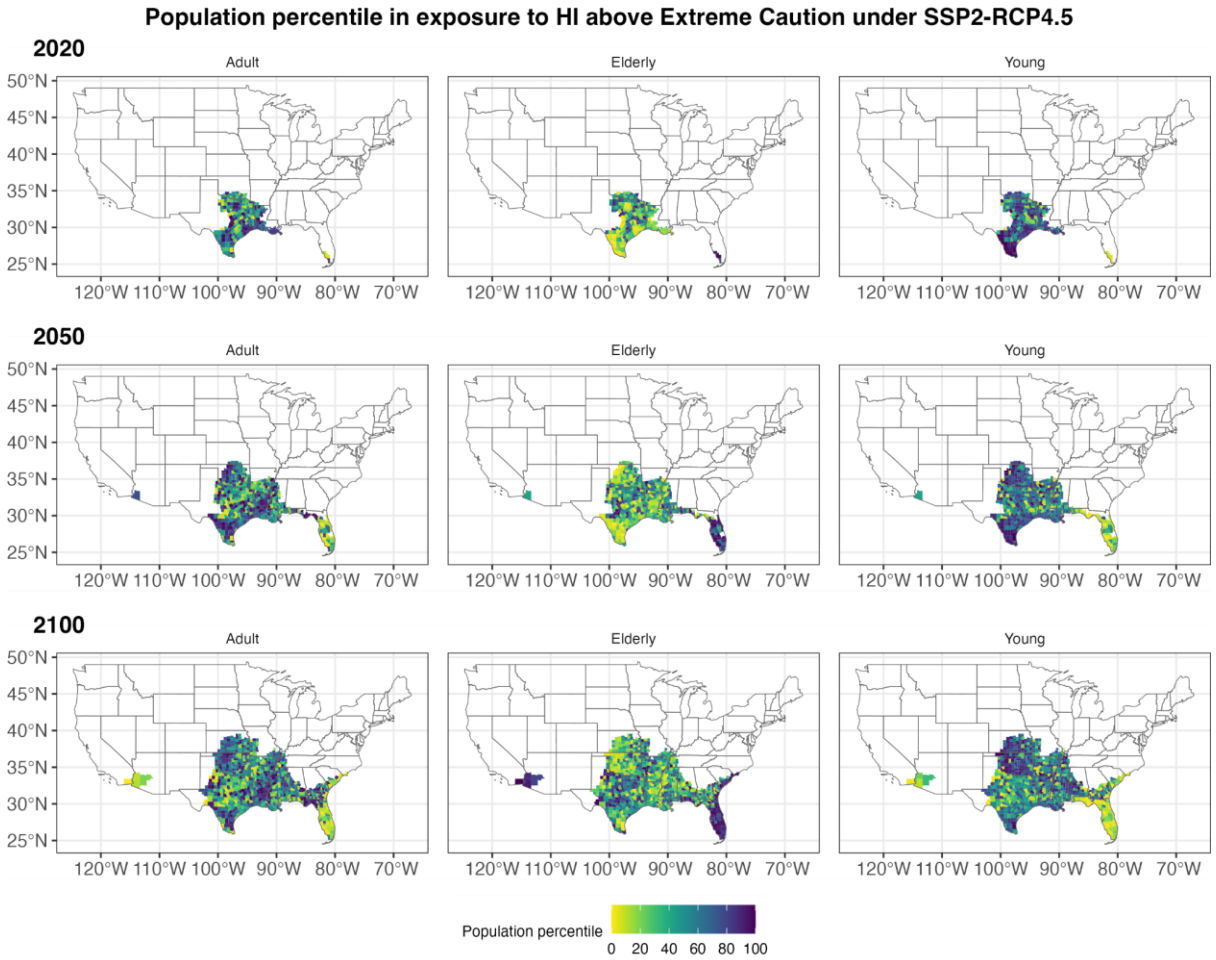

Figure S13 Population percentile of age groups in exposure to HI above Extreme Caution under SSP2-RCP4.5 scenario

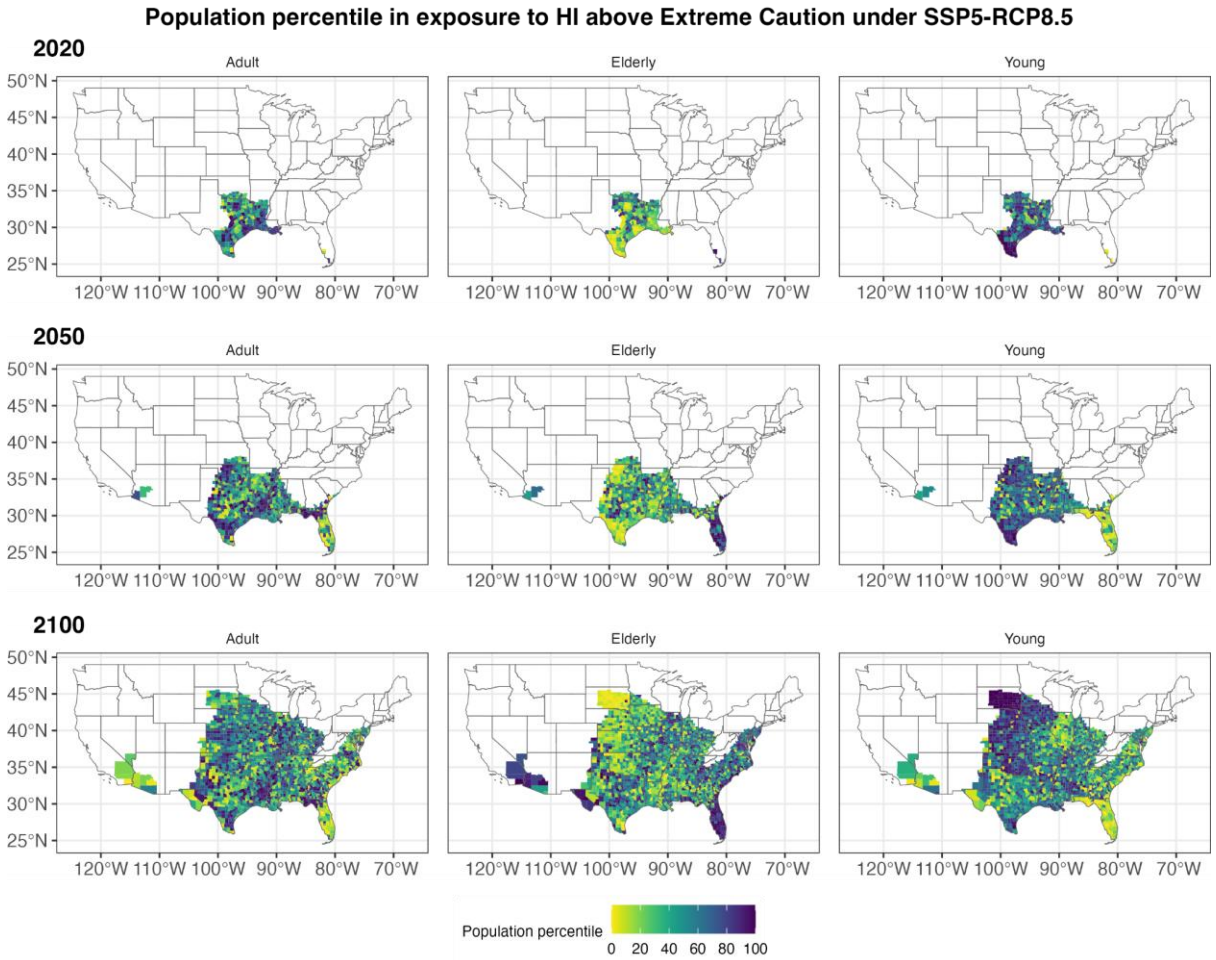

Figure S14 Population percentile of age groups in exposure to HI above Extreme Caution under SSP5-RCP8.5 scenario

Figure S15 Percentage of population exposed to Extreme Caution+ heat risk under coupled SSP-RCP scenarios by age group

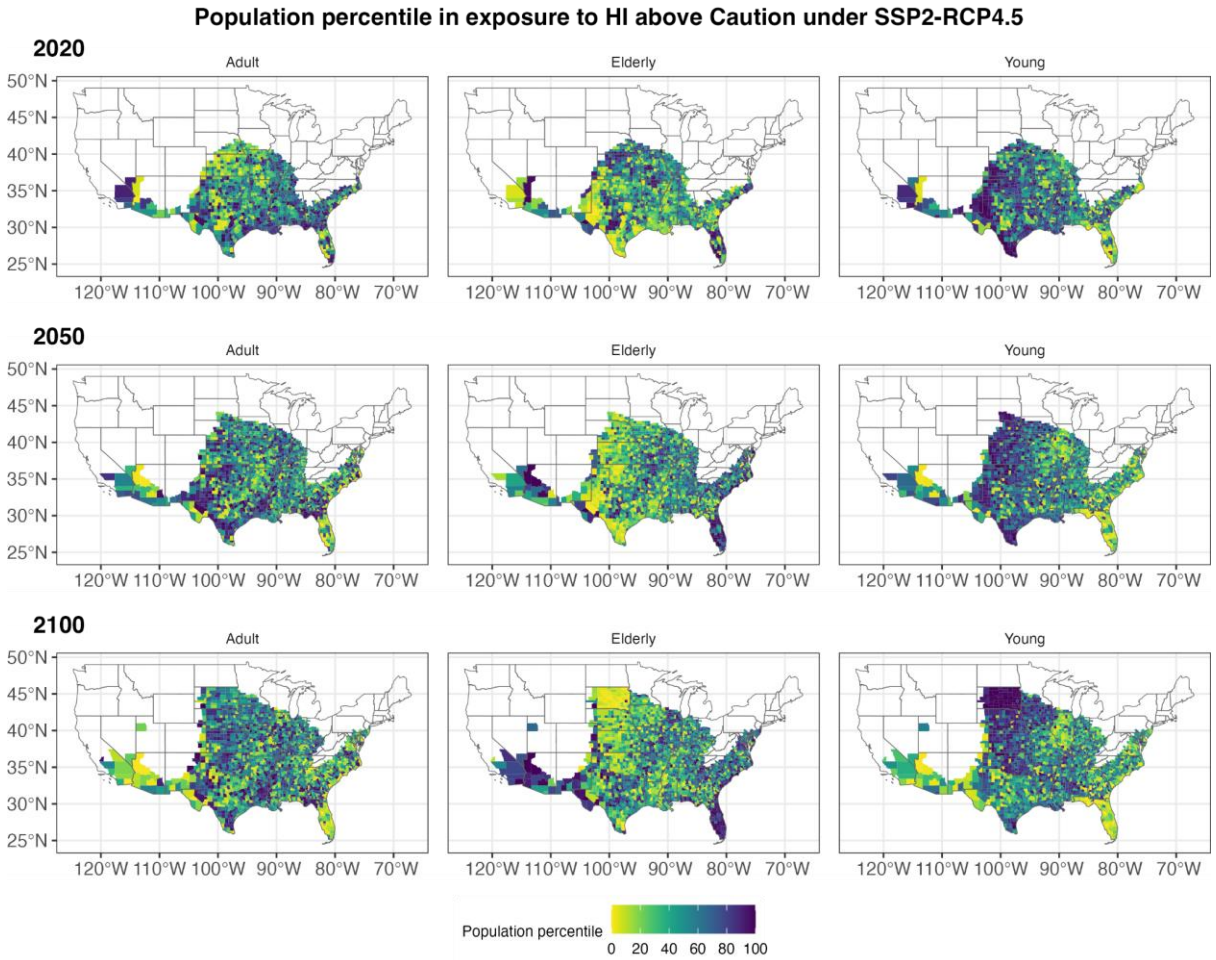

Figure S16 Population percentile of age groups in exposure to HI above Caution under SSP2-RCP4.5 scenario

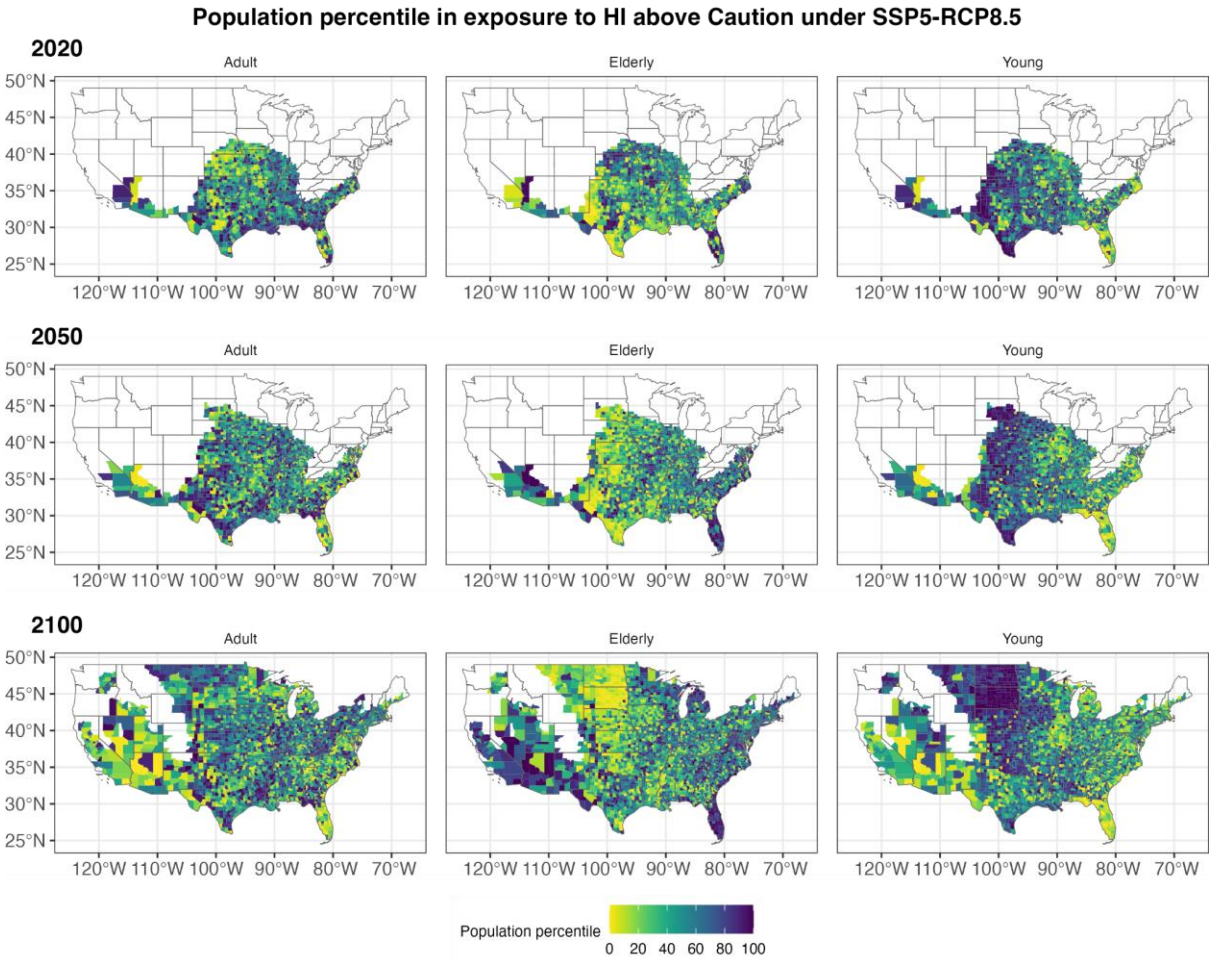

Figure S17 Population percentile of age groups in exposure to HI above Caution under SSP5-RCP8.5 scenario

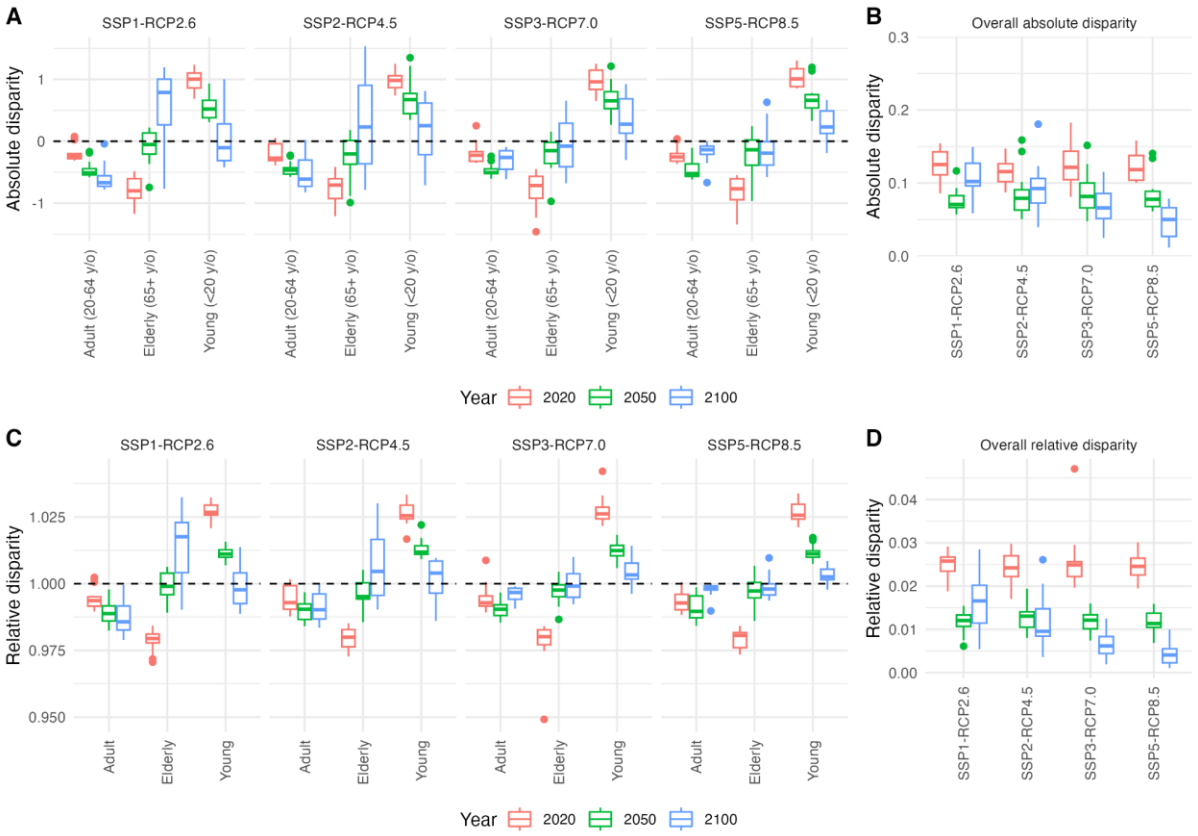

Figure S18 Age disparity in exposure to Heat Index above *Caution* (HI ≥ 80°*F*) threshold. (A) Absolute disparity and relative disparity of age groups in exposure to Heat Index above *Caution* threshold under future scenarios. **(B)** Overall absolute disparity of age groups in exposure to Heat Index above *Caution* threshold under future scenarios; **(C)** Relative disparity of age groups in exposure to Heat Index above *Caution* threshold under future scenarios; **(D)** Overall relative disparity of age groups in exposure to Heat Index above *Caution* threshold under future scenarios. (Note 1: Each box plot shows the interquartile range (25th–75th percentile), with the median indicated by a horizontal line.Whiskers extend to 1.5× the IQR, and points beyond the whiskers are plotted as outliers. Please see Supplementary Information SI1.1 for more details on the number of models. Note 2: The black dash lines represent benchmark values for perfect equalization.)

Figure S19 Percentage of population exposed to Extreme Caution+ heat risk under coupled SSP-RCP scenarios by age group

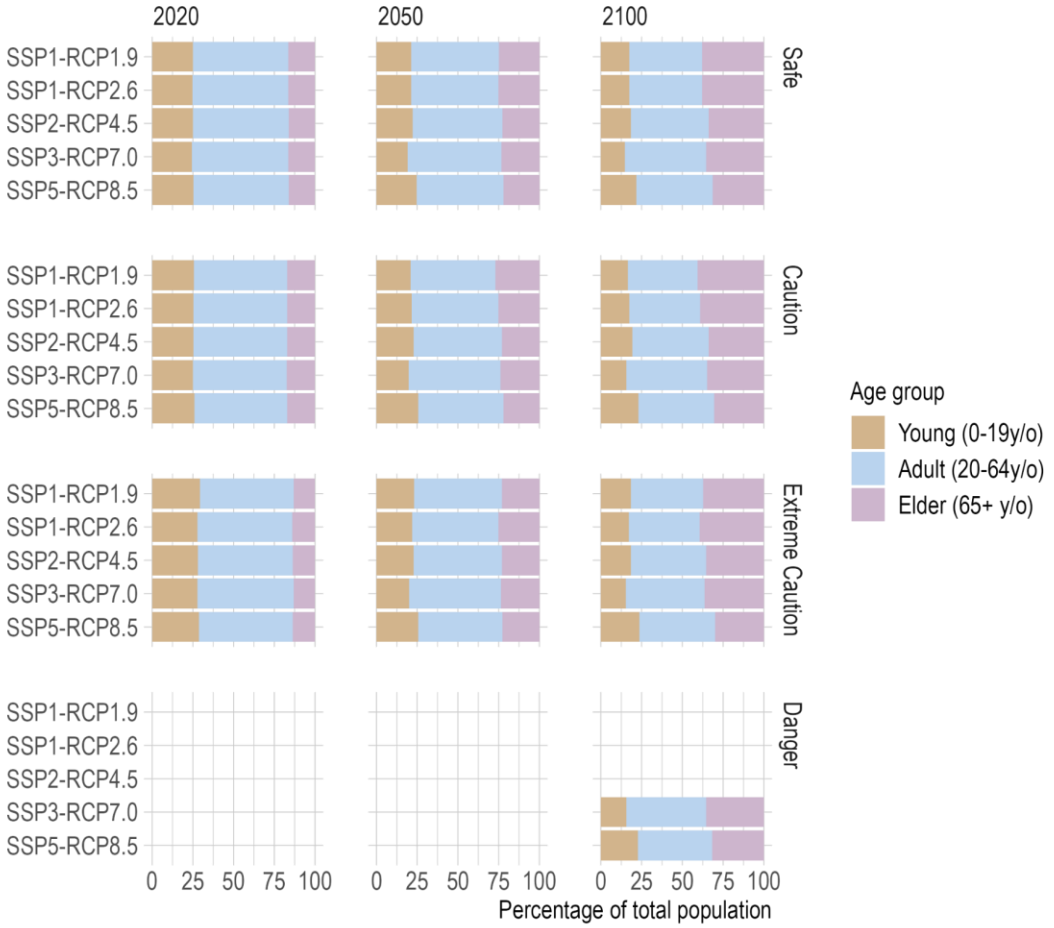

Figure S20 Age composition for each Heat Index zone

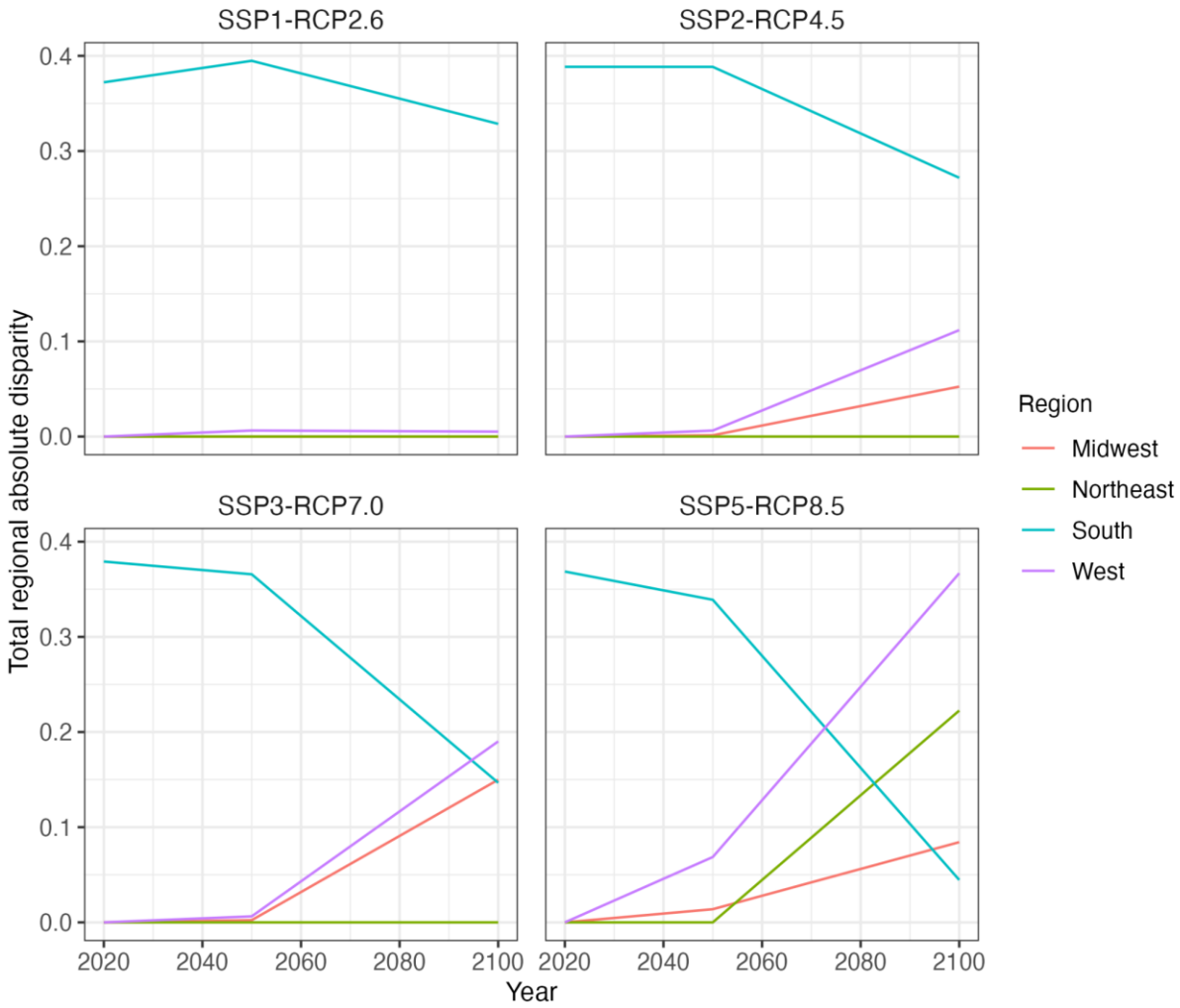

Figure S21 Total racial/ethnic absolute disparity by region

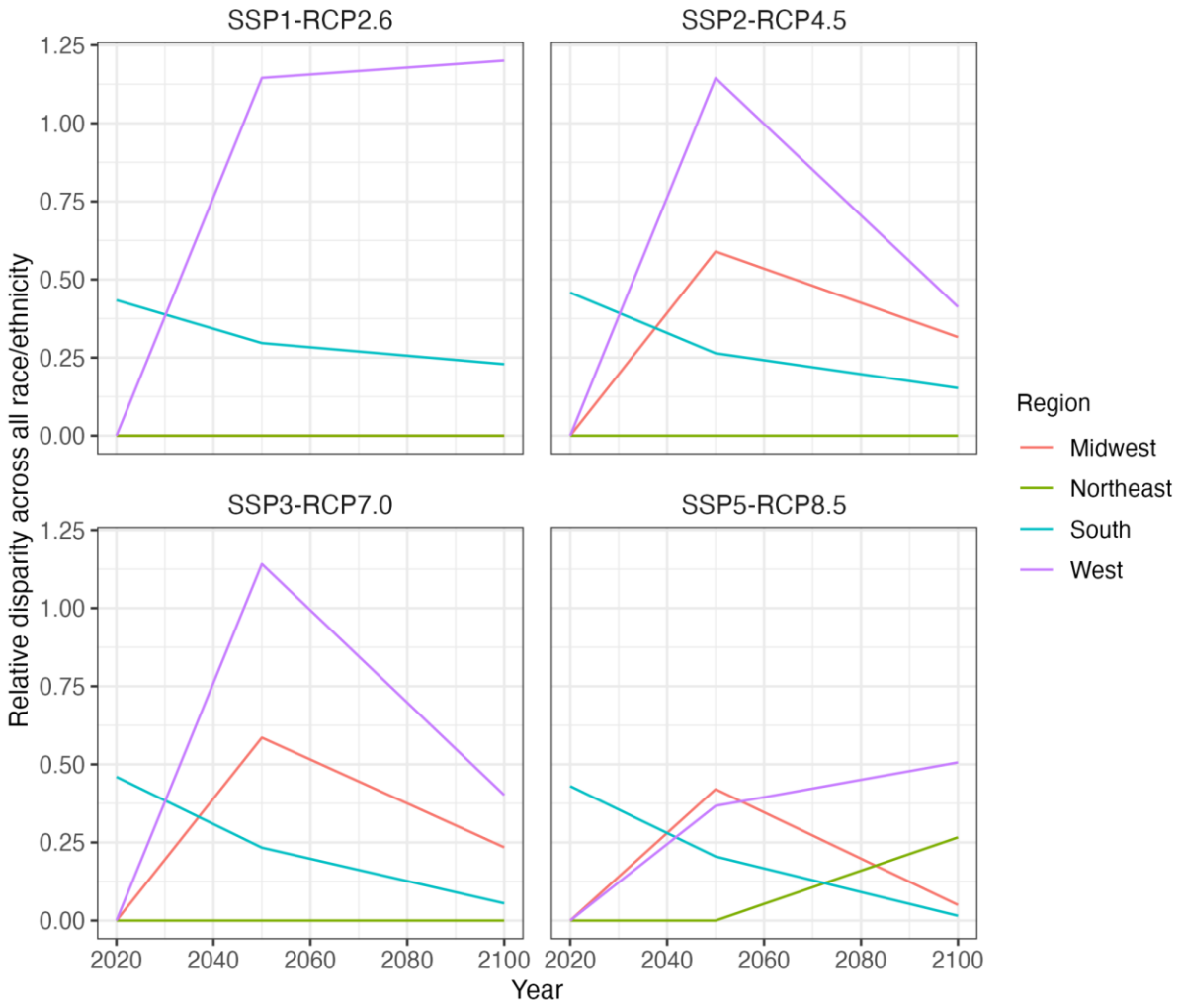

Figure S22 Total racial/ethnic relative disparity by region

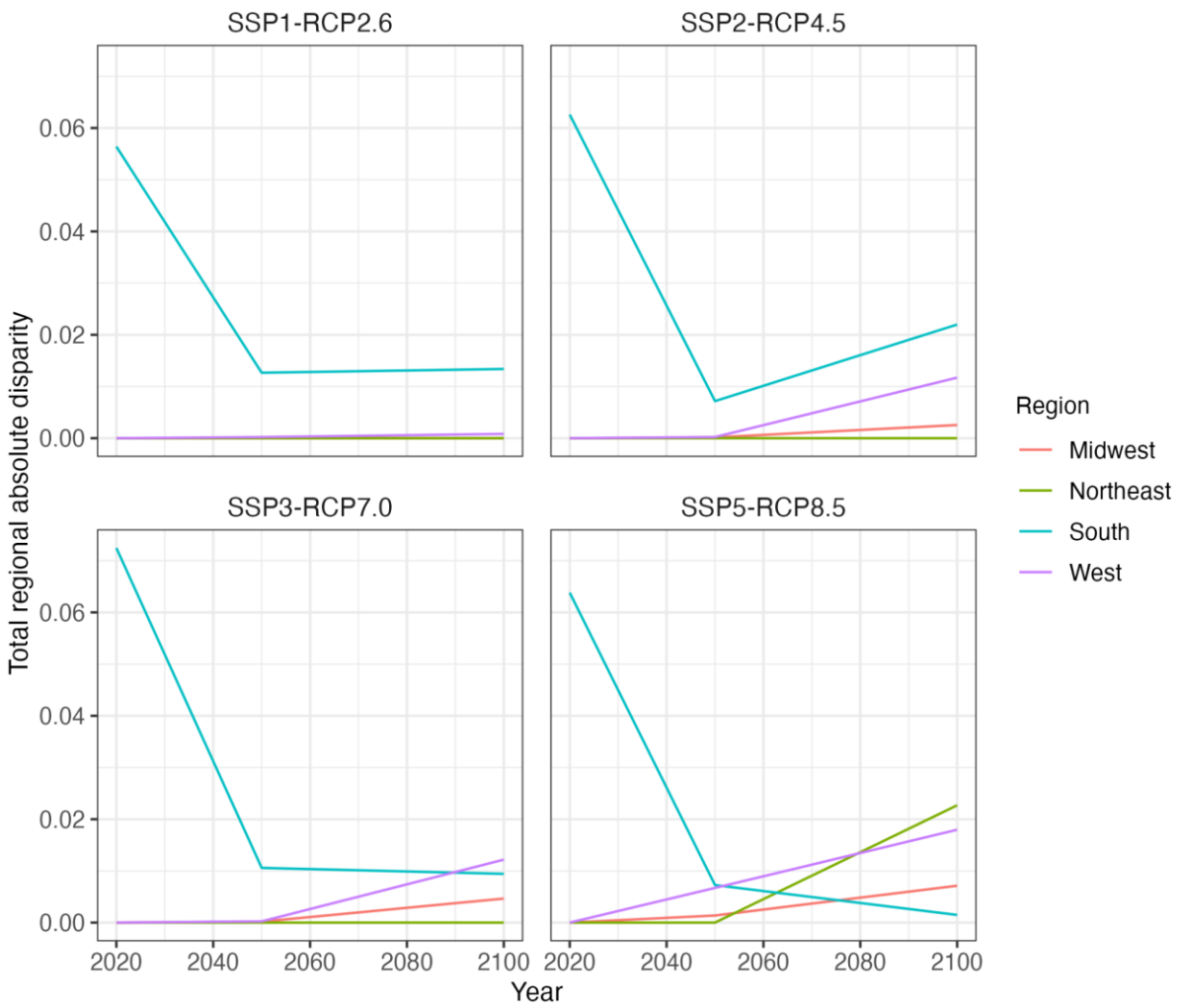

Figure S23 Total age absolute disparity by region

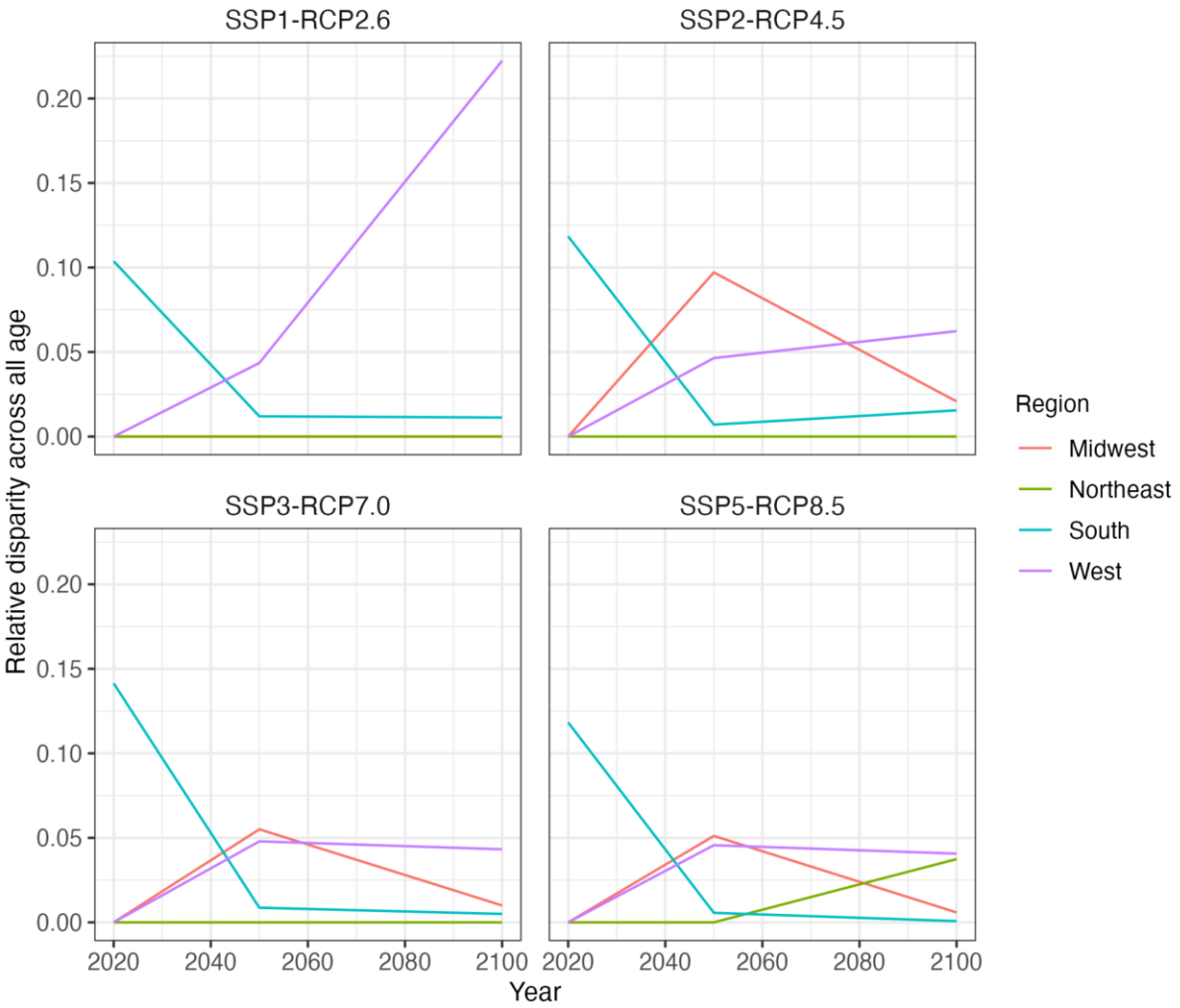

Figure S24 Total age absolute disparity by region

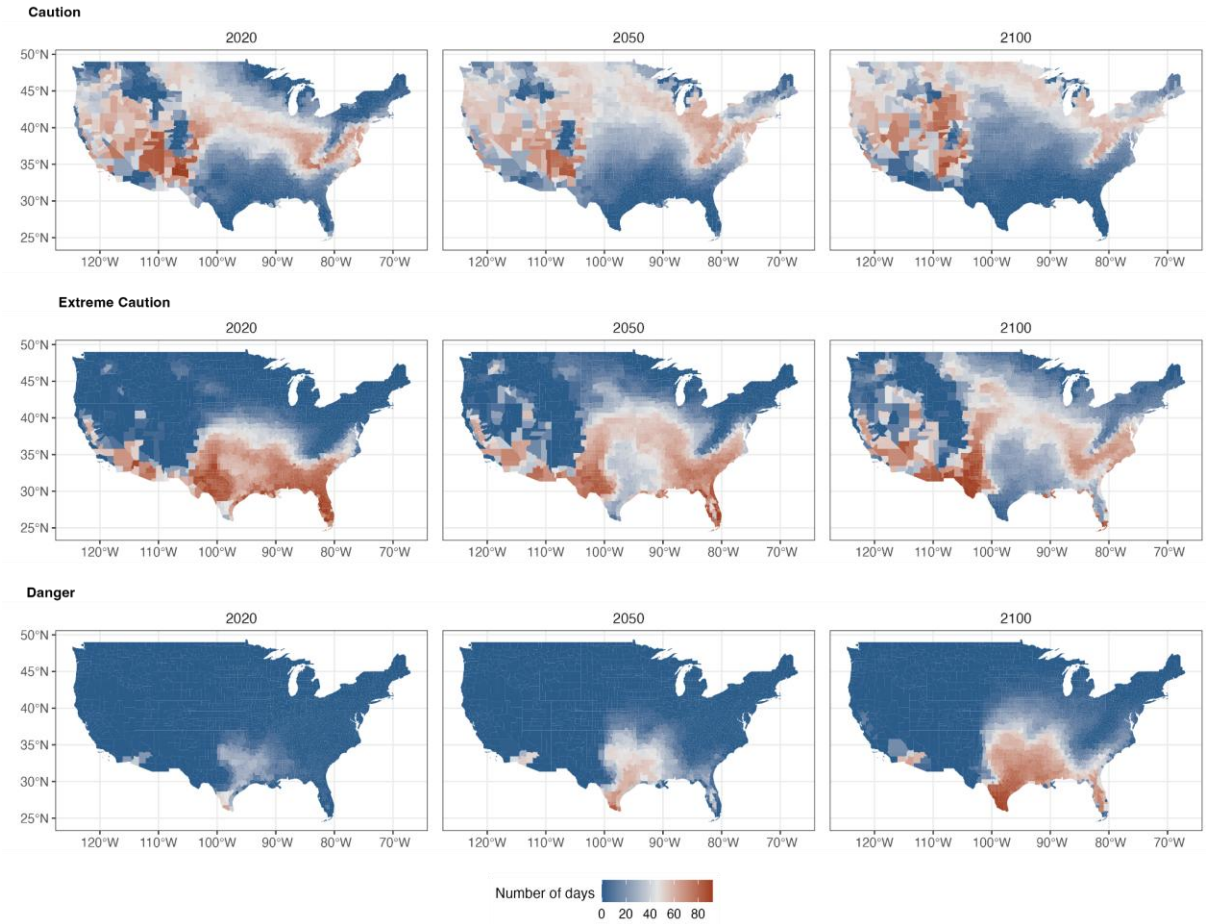

Figure S25 Number of summer days (June–August) at NWS heat-risk thresholds ("Caution," "Extreme Caution," "Danger"). Daily maximum air temperature and daily minimum relative humidity were used to compute daily maximum HI. Values shown are from the EC-Earth3 CMIP6 model under SSP2–RCP4.5, summed across the three months.

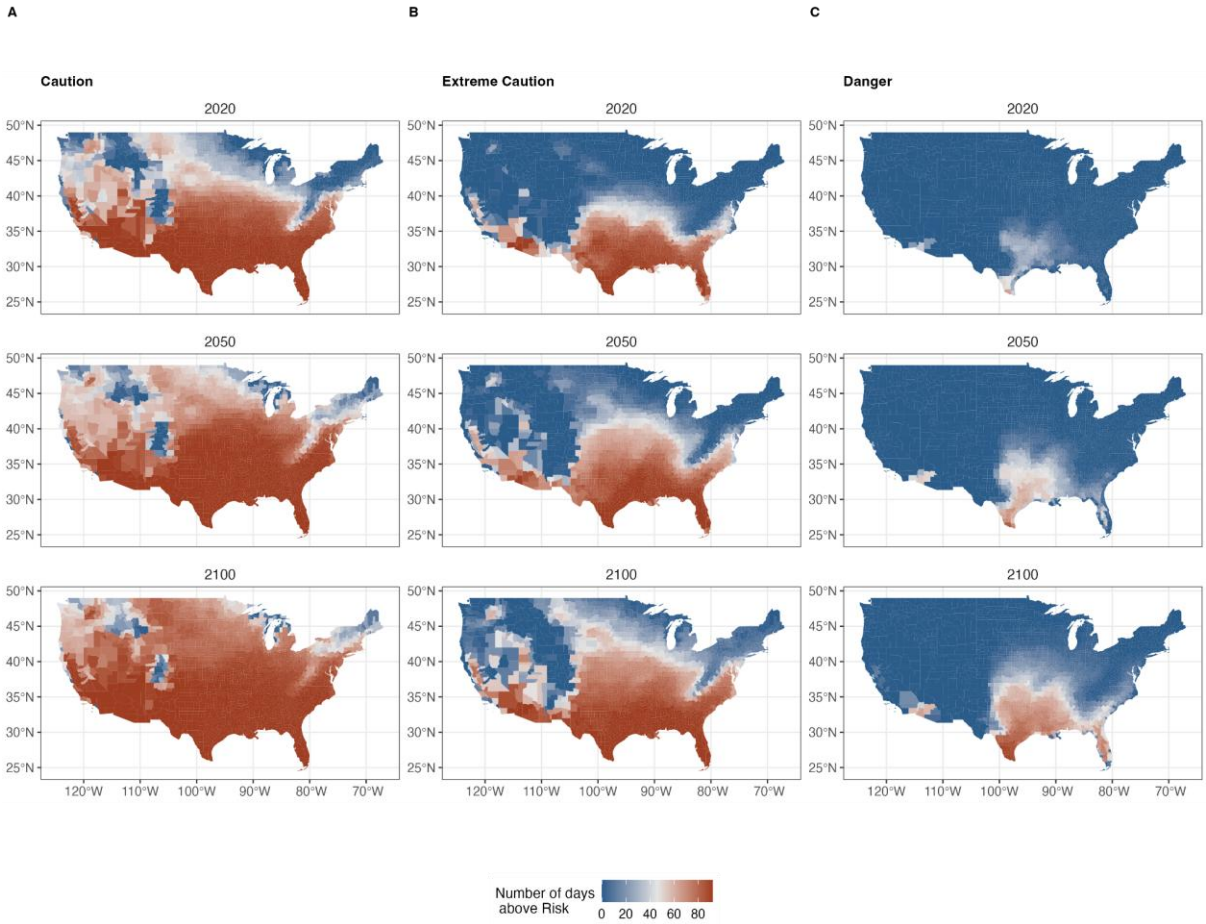

Figure S26 Total number of days exceeding NWS heat-risk thresholds ("Caution," "Extreme Caution," "Danger"). Daily maximum air temperature and daily minimum relative humidity were used to compute daily maximum HI. Values shown are from the EC-Earth3 CMIP6 model under SSP2–RCP4.5, summed across the three months.

disparities of heat risks due to climate change

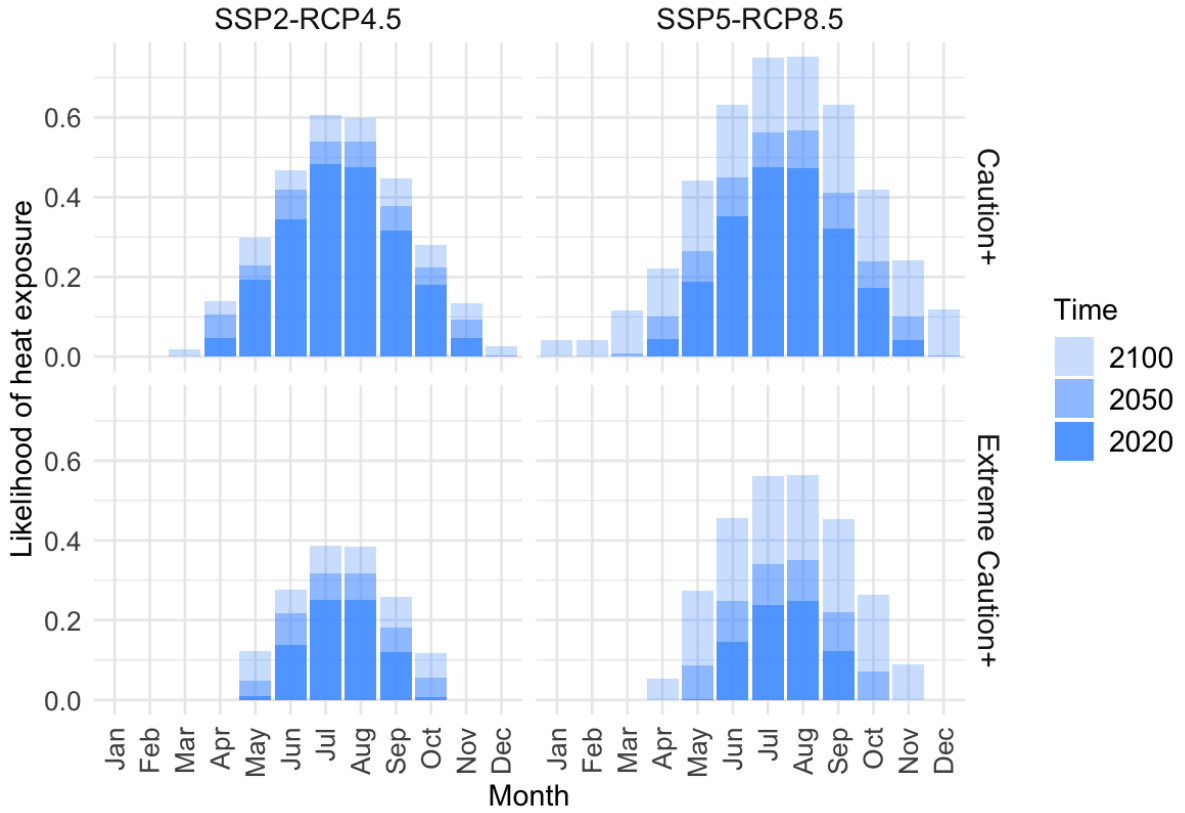

Figure S27 Likelihood of heat exposure for all months under SSP2-RCP4.5 and SSP5-RCP8.5 scenarios in 2020, 2050, and 2100

Supplemental References

1. Tebaldi, C., Debeire, K., Eyring, V., Fischer, E., Fyfe, J., Friedlingstein, P., Knutti, R., Lowe, J., O'Neill, B., Sanderson, B., et al. (2021). Climate model projections from the Scenario Model Intercomparison Project (ScenarioMIP) of CMIP6. Earth Syst. Dyn. *12*, 253–293. https://doi.org/10.5194/esd-12-253-2021.

2. O'Neill, B.C., Tebaldi, C., Vuuren, D.P. van, Eyring, V., Friedlingstein, P., Hurtt, G., Knutti, R., Kriegler, E., Lamarque, J.-F., Lowe, J., et al. (2016). The Scenario Model Intercomparison Project (ScenarioMIP) for CMIP6. Geosci. Model Dev. *9*, 3461–3482. https://doi.org/10.5194/gmd-9-3461-2016.

3. Anderson, G.B., Bell, M.L., and Peng, R.D. (2013). Methods to Calculate the Heat Index as an Exposure Metric in Environmental Health Research. Environ. Health Perspect. *121*, 1111–1119. https://doi.org/10.1289/ehp.1206273.

4. Zhang, K., Cao, C., Chu, H., Zhao, L., Zhao, J., and Lee, X. (2023). Increased heat risk in wet climate induced by urban humid heat. Nature *617*, 738–742. https://doi.org/10.1038/s41586-023-05911-1.

5. Pierce, D.W., Cayan, D.R., Maurer, E.P., Abatzoglou, J.T., and Hegewisch, K.C. (2015). Improved Bias Correction Techniques for Hydrological Simulations of Climate Change*.

J. Hydrometeorol. *16*, 2421–2442. https://doi.org/10.1175/JHM-D-14-0236.1.

6. Dahl, K., Licker, R., Abatzoglou, J.T., and Declet-Barreto, J. (2019). Increased frequency of and population exposure to extreme heat index days in the United States during the 21st century. Environ. Res. Commun. *1*, 075002.

7. Gao, J., and Pesaresi, M. (2021). Downscaling SSP-consistent global spatial urban land projections from 1/8-degree to 1-km resolution 2000–2100. Sci. Data *8*, 281. https://doi.org/10.1038/s41597-021-01052-0.

8. Hauer, M.E. (2019). Population projections for U.S. counties by age, sex, and race controlled to shared socioeconomic pathway. Sci. Data *6*, 190005. https://doi.org/10.1038/sdata.2019.5.

9. Murakami, D., Yoshida, T., and Yamagata, Y. (2021). Gridded GDP Projections Compatible With the Five SSPs (Shared Socioeconomic Pathways). Front. Built Environ. *7*. https://doi.org/10.3389/fbuil.2021.760306.

10. Ballester, J., Quijal-Zamorano, M., Méndez Turrubiates, R.F., Pegenaute, F., Herrmann, F.R., Robine, J.M., Basagaña, X., Tonne, C., Antó, J.M., and Achebak, H. (2023). Heat-related mortality in Europe during the summer of 2022. Nat. Med. *29*, 1857–1866. https://doi.org/10.1038/s41591-023-02419-z.

11. Wang, J., Chen, Y., Tett, S.F.B., Yan, Z., Zhai, P., Feng, J., and Xia, J. (2020). Anthropogenically-driven increases in the risks of summertime compound hot extremes. Nat. Commun. *11*, 528. https://doi.org/10.1038/s41467-019-14233-8.

12. Esper, J., Torbenson, M., and Büntgen, U. (2024). 2023 summer warmth unparalleled over the past 2,000 years. Nature *631*, 94–97. https://doi.org/10.1038/s41586-024-07512-y.